國立交通大學

資訊工程系

碩 士 論 文

應用在 IEEE 802.11g 上頻域等化與資料解碼的結合

Combination with Frequency Domain Equalization and Data Demapping

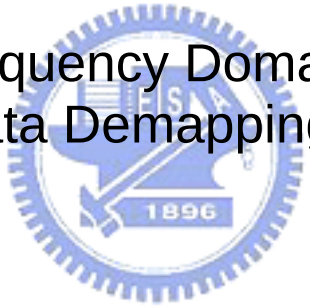

研 究 生：蔡爵安

指導教授：許騰尹　博士

中 華 民 國 九 十 四 年 八 月

應用在 IEEE 802.11g 上頻域等化與資料解碼的結合
Combination with Frequency Domain Equalization and Data Demapping

研 究 生：蔡爵安　　Student：Chueh-An Tsai

指導教授：許騰尹 博士　　Advisor：Dr. Terng-Yin Hsu

國 立 交 通 大 學

資 訊 工 程 系

碩 士 論 文

A Thesis

Submitted to Department of Computer Science and Information Engineering

College of Electrical Engineering and Computer Science

National Chiao Tung University

in partial Fulfillment of the Requirements

for the Degree of

Master

in

Computer Science and Information Engineering

August 2005

Hsinchu, Taiwan, Republic of China

中華民國九十四年八月

Combination with Frequency Domain Equalization and Data Demapping

Student：Chueh-An Tsai Advisors：Dr. Terng-Yin Hsu

Department of Computer Science and Information Engineering,
National Chiao Tung University

ABSTRACT

A procedure against heavy multipath is developed in this thesis, which combines equalization with CCK codewords demapping and is based on conditioned maximum likelihood (ML) criterion in frequency domain by means of only one DFT. These techniques is applied to dual mode system IEEE 802.11g so that ERP-DSSS/CCK mode can share DFT and point by point multiplier of ERP-OFDM mode and reach the purpose of hardware saving, instead of huge DFE in most solutions of IEEE 802.11g ERP-DSSS/CCK mode. However, 802.11g systems are now being used in home, office and warehouse environments where the multipath delay can be much greater on the order of about 150ns. Such environments require the use of equalization for acceptable performance. According to simulation results under IEEE 802.11g and JTC indoor multipath models, the concepts of joint equalization and CCK demapping not only provide acceptable accomplishment but also improve the performance of the system substantially over separate equalization and demapping.

Contents

Abstract

Contents

1 Introduction 1

2 Platform and Simulation Environments 3

2.1 Platform Specification & Transmitter 3

2.2 Channel Model & Signal Modeling 5

2.3 Receiver. 10

3 Channel Estimation & Equalization 13

3.1 Channel Estimation 13

3.1.1 Proposed Scheme #1 14

3.1.2 Proposed Scheme #2 21

3.1.3 Comparison 29

3.2 Equalization 30

3.2.1 Previous Remark 30

3.2.2 Frequency Domain Equalization Combined with Data Demapping 30

4 Simulation Results 39

4.1 Channel Estimation Scheme #1 with Proposed Demapper 39

4.2 Channel Estimation Scheme #2 with Proposed Demapper 41

5 Conclusion and Future Works 45

5.1 Conclusion 45

5.2 Future Works 45

Bibliography

Appendix JTC indoor channel model profile

Chapter 1

Introduction

As a mobile-computing era has come, wireless LAN is regarded as an effective technology that enables people to do it because of its mobility and flexibility. IEEE 802.11b [1] system, which is almost dominant at present, has transmitting speed that is insufficient for multimedia data. To overcome ifs speed problem, IEEE 802.11a standard [2] that has the maximum speed of 54 Mbps in 5 GHz band has been developed recently. But most companies had already installed 802.11b systems, and so want a new standard that complies with existing 802.11b systems. To meet this demand, IEEE 802.11g standard [3] has been established from 2001. It is capable of operating in any of available modes such as ERP (Extended Rate PHY)-DSSS/CCK (Complementary Code Keying), ERP-OFDM (Orthogonal Frequency Division Multiplexing), Extended Rate PBCC (Packet Binary Convolutional Coding), and CCK-OFDM. It offers various data rates from 1 Mbps to 54 Mbps in 2.4 GHz band, and handles DBPSK, DQPSK, QPSK, 8-PSK, BPSK, 16-QAM, and 64-QAM modulation schemes. It also has better signal transmitting ability compared with 802.11a using 5GHz band, and complies with existing 802.11b systems. These are just the reason that 802.11g is an interesting and important topic.

With trend of integration over standards (from IEEE 802.11a, 11b to 11g), this thesis presents a baseband solution of dual mode equalization on platform for wireless LAN system complies with the 802.11g standard. It can operate in main physical modes proposed in the 802.11g standard, namely ERP-DSSS/CCK and ERP-OFDM, and it can be regard as a dual mode system. The proposed method performs a possibility of sharing the same function blocks that work for ERP-DSSS/CCK and ERP-OFDM in order to reduce hardware implementation cost,

and overcomes the difference between different domain equalization at the same time. In chapter 2, we not only introduce specifications of IEEE 802.11g but also describe why we choose frequency domain as our major equalization domain, and the relative block diagram is shown. In chapter 3, two frequency-domain channel estimation schemes are proposed without aliasing effect with regard to ERP-DSSS/CCK mode. Then, a frequency domain conditional maximum likelihood (CML) demapping that combines equalization with decoding is developed according to estimated channel frequency response (CFR) as well. Chapter 4 presents simulation results of two channel estimation schemes with proposed CML demapping under different operating rate and channel model, and conclusion is given as well in chapter 5.

Chapter 2

Platform and Simulation Environments

This chapter is going to describe complete simulation environments from IEEE 802.11g PHY specifications (transmitter), wireless effects to baseband receiver. The 802.11g can roughly be regarded as the combination of IEEE standards 802.11a and 802.11b, and thus, an 802.11g device is available to previous 802.11b or 802.11a devices. All is divided to several sections. The 802.11g PHY specifications and transmission architectures will be introduced; wireless channel models and parameters of environment will be defined, too. The last section will dwell on the solutions to baseband receiver architectures, where an intuitive, general method and a proposed one with concept of module sharing are listed. Clearly, advanced discussions and simulation results in chapter 3 and 4 is based on the proposed receiver.

2.1 Platform specification & transmitter

The 802.11g PHY defined in standard is known as the Extended Rate PHY (ERP), operating in the 2.4 GHz ISM band. Four operational modes is as followed:

a) ERP-DSSS/CCK – This mode builds on the payload data (PSDU) rates of 1, 2, 5.5, and 11 M bit/s that use DSSS (DBPSK and DQPSK), CCK and optional PBCC modulation, and the PLCP Header operates on data rate 1 M bit/s DBPSK for Long SYNC, 2 M bit/s DQPSK for Short SYNC. Figure 2.1 shows the format for the interoperable PPDU that is the same with 802.11b PPDU format, and the details of components such as spreading code, scrambler, CRC implementation, and modulation refer to 802.11b standard.

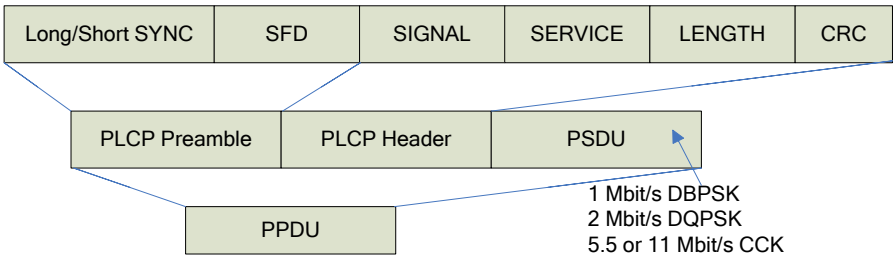

Figure 2.1 ERP-DSSS/CCK PPDU format

b) ERP-OFDM – This mode builds on the payload data rates of 6, 9, 12, 18 24, 36, 48, and 54 M bit/s, based on different modulations (PSK and QAM) and coding rate, by means of OFDM technique. Except PLCP Preamble, SIGNAL field with data rate 6 M bit/s and DATA are packaged (OFDM) symbol by symbol. The only difference from 802.11a is the operating ISM band (802.11a is in 5 GHz). Figure 2.2 is the PPDU format.

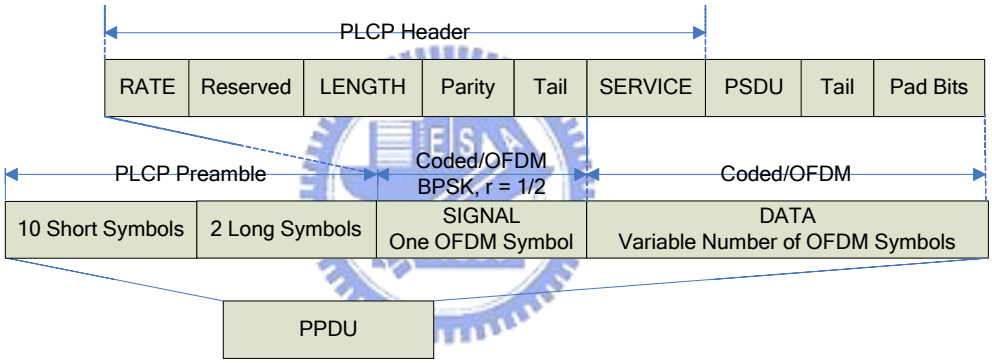

Figure 2.2 ERO-OFDM PPDU format

c) ERO-PBCC – This mode builds on the payload data (PSDU) rates of 22 and 33 M bit/s and it is a single-carrier modulation scheme that encodes the payload using 256-state packet binary convolutional code. The PPDU format follows mode a).

d) DSSS-OFDM – This mode is a hybrid modulation combining a DSSS preamble and header with an OFDM long preamble, signal field and payload transmission. In the boundary between DSSS and OFDM parts, it is single carrier to multicarrier transition definition. The payload data rates are the same with those of b). The PPDU format is as followed,

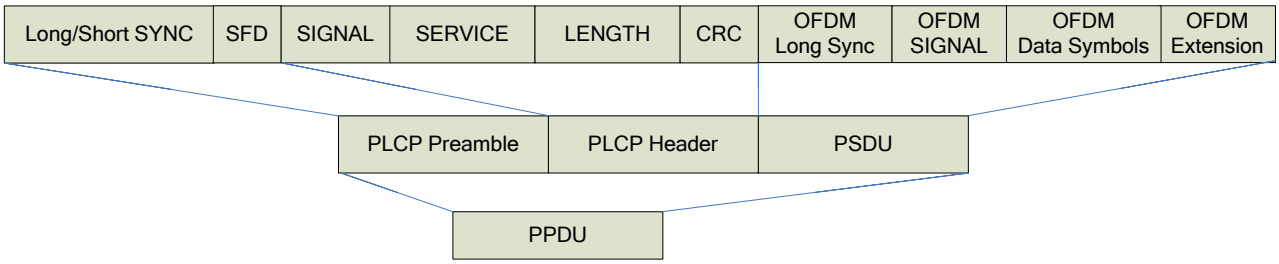

Figure 2.3 DSSS-OFDM PPDU format

An ERP BSS is capable of operating in any combination of available ERP modes and Non-ERP modes. For example, if options are enabled, a BSS could operate in an ERP-OFDM-only mode, a mixed mode of ERP-OFDM and ERP-DSSS/CCK, or a mixed mode of ERP-DSSS/CCK and Non-ERP. Notice that since the first two modes are required to implement and considered as main operating modes and the others are optional, the discussion of platform will be located on the first two modes hereinafter.

Figure 2.4 is the transmitter block diagram. After the parameters of operation mode, data rate and data length are decided, following these blocks one by one will generate the transmitted signals, and the MUX that depends on operation mode will select the signal that be sent to air by antenna after up-conversioning the baseband signals to operating channel frequency.

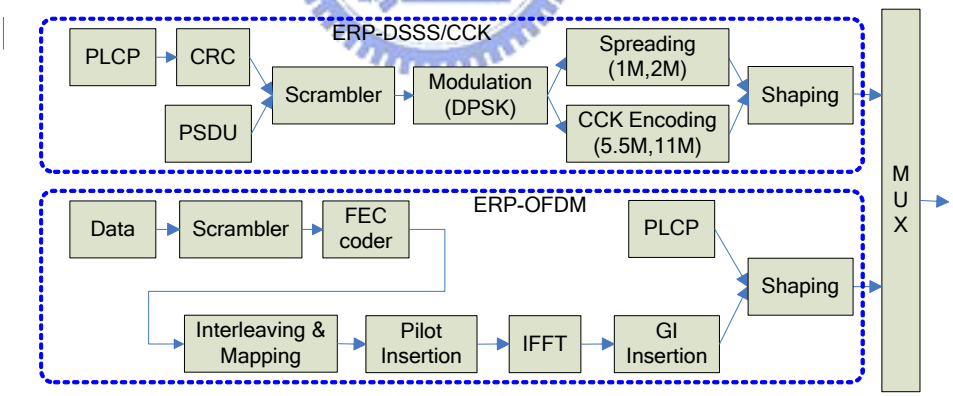

Figure 2.4 transmitter block diagrams

2.2 Channel models

For wireless communication system, because air is the medium for transmission, the wireless channel models are more complicated than wired ones. Many irresistible atmosphere factors have to be put into consideration. From the transmitter end to receiver end, that baseband signals are masked within transmit spectrum mask that

is defined in standards, that signal power decreases with the distance between transmitter and receiver, that the signals are convolved with multipath, which means signals are affected significantly by their delay version, that signals are added with AWGN, and that carrier frequency offset is multiplied to signals with time index, are explained particularly as below:

a) Transmit spectrum mask:

It is well-known to use raised cosine spectrum as the shaping filter that fits the transmit spectrum mask in standard. The raised cosine frequency characteristic is given as

$$X_{rc}(f)=\begin{cases} T & \left(0\le|f|\le\dfrac{1-\beta}{2T}\right) \\ \dfrac{T}{2}\left\{1+\cos\left[\dfrac{\pi T}{\beta}\left(|f|-\dfrac{1-\beta}{2T}\right)\right]\right\} & \left(\dfrac{1-\beta}{2T}\le|f|\le\dfrac{1+\beta}{2T}\right) \\ 0 & \left(|f|>\dfrac{1+\beta}{2T}\right) \end{cases} \quad (2.1)$$

where β is called the roll-off factor and takes values in the range $0\le\beta\le1$. The roll-off factor is the percentage of the bandwidth occupied by signal beyond the Nyquist frequency ($1/T$) to the Nyquist frequency. For example, when β=0.5, the excess bandwidth is 50 percent of $1/T$. The corresponding impulse $x_{rc}(t)$, having the raised cosine spectrum and is normalized, is

$$x_{rc}(t)=\frac{\sin(\pi t/T)}{\pi t/T}\cdot\frac{\cos(\pi\beta t/T)}{1-4\beta^2t^2/T}=\sin c(\pi t/T)\cdot\frac{\cos(\pi\beta t/T)}{1-4\beta^2t^2/T} \quad (2.2)$$

If sample timing is correct, all samples will avoid inter-symbol interference (ISI) due to raised cosine function; if not, mistiming errors in sampling result in a series of ISI components that converges to a finite value.

b) Path loss:

Path loss is the difference (usually measured in dB) between the transmitted power and the received power. It represents signal level attenuation caused by free-space loss, refraction, reflection, aperture-medium coupling loss, and absorption. At the receiver, it is necessary to implement a variable gain amplifier (VGA) to enhance signal power and a controller, called automatic gain control (AGC), to estimate proper path loss parameter and justify the VGA gain.

This topic was discussed deeply in [4].

c) Multipath:

Because there are obstacles and reflectors in the wireless propagation channel, the transmitted signal arrivals at the receiver from various directions over a multiplicity of paths. Such a phenomenon is called multipath. It is an unpredictable set of reflections and/or direct waves each with its own degree of attenuation and delay. Multipath is usually described by two sorts:

1) Line-of-sight (LOS): the direct connection between the transmitter (TX) and the receiver (RX).
2) Non-line-of-sight (NLOS): the path arriving after reflection from reflectors.

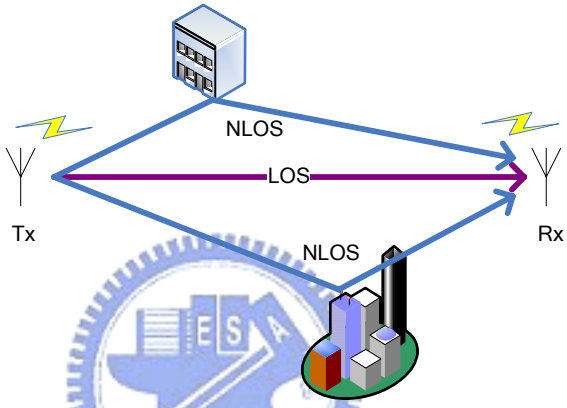

Figure 2.5 LOS and NLOS

Multipath will cause amplitude and phase fluctuations, and time delay in the received signals. When the waves of multipath signals are out of phase, reduction of the signal strength at the receiver can occur. One such type of reduction is called the multipath fading; the phenomenon is known as "Rayleigh fading" or "fast fading." A representation of Rayleigh fading and a measured received power-delay profile are shown in Figure 2.6. Besides, multiple reflections of the transmitted signal may arrive at the receiver at different times; this can result in inter-symbol interference that the receiver cannot sort out. This time dispersion of the channel is called multipath delay spread that is an important parameter to access the performance capabilities of wireless systems. A common measure of multipath delay spread is the root mean square (RMS) delay spread. For a reliable communication without using adaptive equalization or other anti-multipath techniques, the transmitted data rate should be much smaller than the inverse of the RMS delay spread (called coherence bandwidth). And, this paper is going to consult some well-known wireless indoor models—

SPW, IEEE 802.11g and JTC multipath models— and provide solutions to system suffered from severe multipath fading mainly.

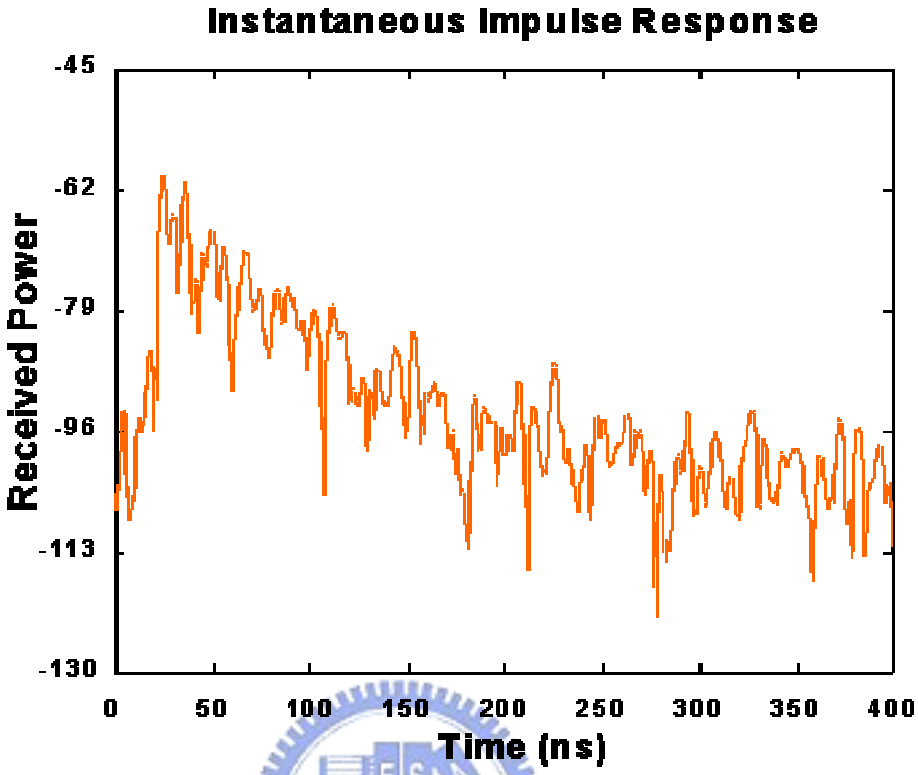

Figure 2.6 measured power-delay profile of Rayleigh fading

d) IQ mismatch:

For phase and frequency modulation scheme, a homodyne receiver must incorporate quadrature mixing. The errors in nominally 90 degrees phase shift, and mismatches between the amplitudes of the I and Q signals corrupt the downconverted signal constellation, thereby raising the bit error rate. Figure 2.7(a) shows that both of I and Q contribute gain and phase error, and Figure 2.7(b) is an example of gain and phase error for QPSK. The details of compensation mechanism have been handled by [5].

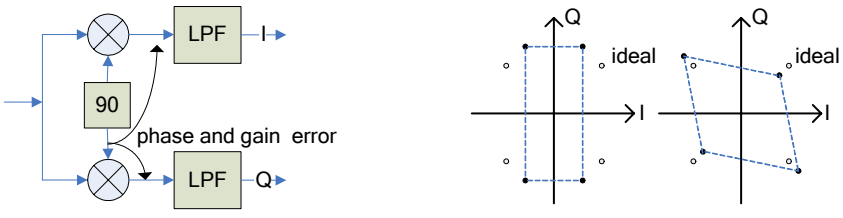

(a) (b)

Figure 2.7 IQ mismatch

e) Carrier frequency offset (CFO)

Ideally, the receiver carrier frequency should exactly match the transmit carrier frequency. However, it is inappropriate in practical application, and the inconsistency between transmitter and receiver oscillators causes CFO, which, in general, is measured in ppm (parts per million). The effect of frequency offset in time domain is equivalent to phase rotation with time, and is compensated by numerically controlled oscillator (NCO) whose parameter is estimated by automatic frequency control (AFC), which is designed in [4] and [6].

All mentioned channel factors that occur over transmission in Figure 2.8 would be bound into our platform parameters. However, this modeling includes bandpass system, thus making difficulty and ambiguity in program simulation. A baseband equivalent model is now derived and is defined in Figure 2.9, where the signal modeling is therefore formulated as

$$r(t) = p(t) \cdot \left[s(t) \otimes g(t) \right] \otimes h(t) \cdot e^{-j\theta(t)} + n(t) \tag{2.3}$$

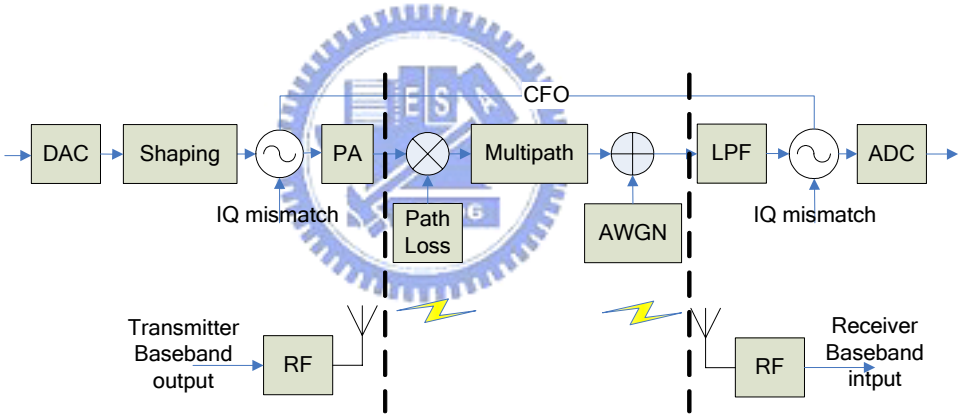

Figure 2.8 channel models

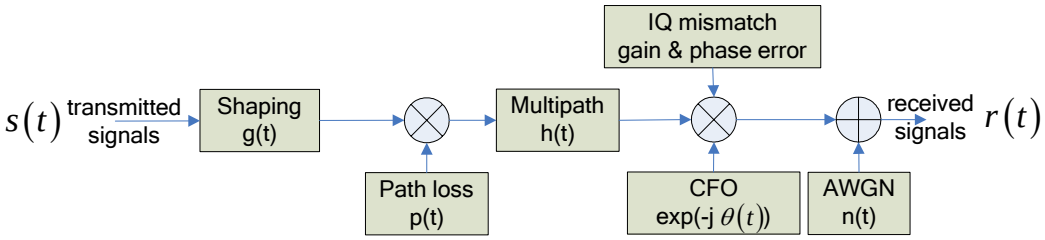

Figure 2.9 baseband equivalent channel models

As the target described in the beginning, our focus will be located on the estimation of $h(t)$ and the equalization of data in chapter 3. We start our research on multipath effect and AWGN noise as most papers did. After T_s-spaced sampling, the

discrete-time received signal is the linear convolution of transmitted signal $x[k]$ and multipath, given by

$$y[k] = y(kT_s) = \sum_{l=0}^{L_h} h[l]x[k-l] + n[k] \tag{2.4}$$

for each packet, with the discrete-time multipath impulse response $h[l] = h(lT_s)$ (L_h is the order of discrete-time multipath model).

2.3 Receiver

For dual-mode 802.11g transmitter, it is directly perceived through the senses that integrate 802.11a and 802.11b receivers with a multiplexer as shown in Figure 2.10. Obviously, there are many modules with the same function, including ADC,

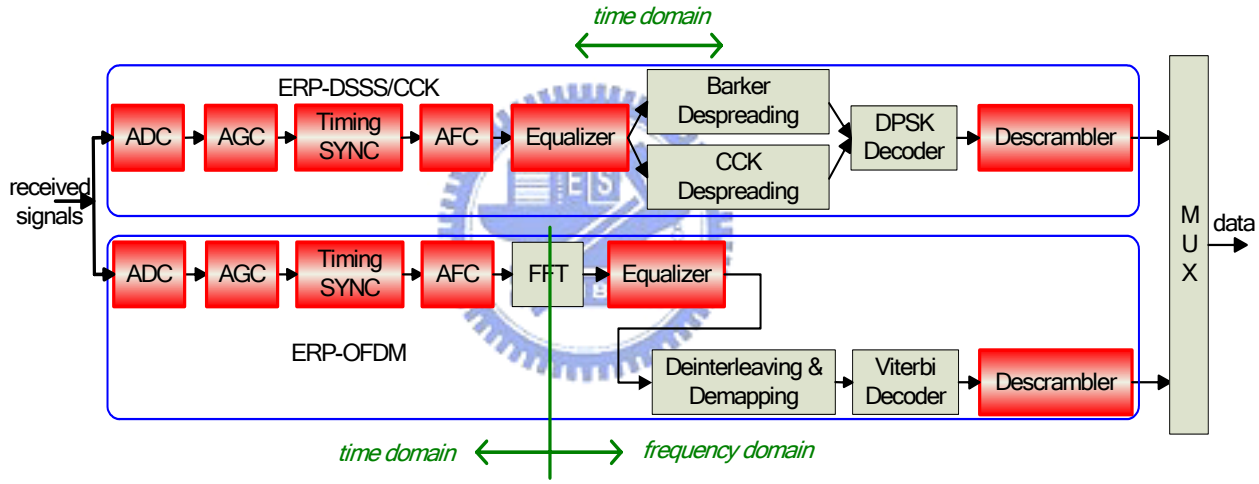

Figure 2.10 separate receiver block diagrams

AGC, Timing SYNC, AFC, Equalizer, and Descrambler. These module blocks are necessary for any type of wireless communication system, which inspiring us to consider a possibility of universal receiver. Because the blocks before FFT operate in time domain no matter DSSS or OFDM system, it is easy to reach the goal of sharing only by means of adding control signals to distinguish different transmission modes. However, equalization, generally, acts in time domain for DSSS system, and in frequency domain for OFDM system. In order to achieve the goal of unique equalizer, it is necessary to choose a domain to conduct interfered signal. Review the equalization of OFDM system; it needs only one divider to deal with convolved time domain signals in frequency domain according to known or estimated channel frequency response. For consideration of time domain solution, not only will

hardware cost with regard to OFDM system increase, but also signal is hard to make decision over original frequency response in time domain. Compared frequency domain solutions with often seen time domain ones, decision feedback equalizer (DFE) or adaptive method, operations with only one divider actually save a lot of hardware cost and computational complexity. Therefore, we proposed a equalizer based on receiver block diagrams as Figure 2.11, which takes OFDM system as the major and DSSS system as the minor, i.e., besides OFDM signal, DSSS signal would be passed through FFT. And to avoid additional IFFT that transform DSSS signal back to time domain, procedures of dispreading and demapping has to be done in frequency domain, too. In other words, we would get rid of common solution, FWT, and give a new frequency domain solution.

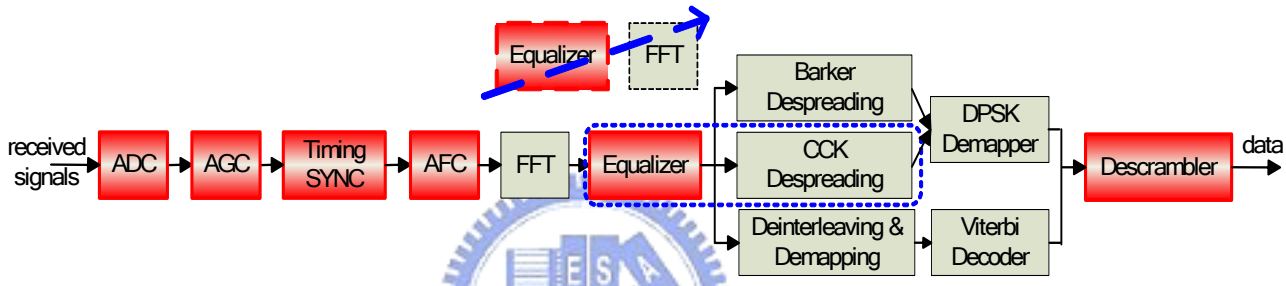

Figure 2.11 universal-directed receiver block diagrams

The challenge is that there is no mechanism that is designed against or to solve multipath effect in DSSS packet format; on the contrary, guard interval of OFDM system result in circular convolution so that deconvolution can be achieved by FFT.

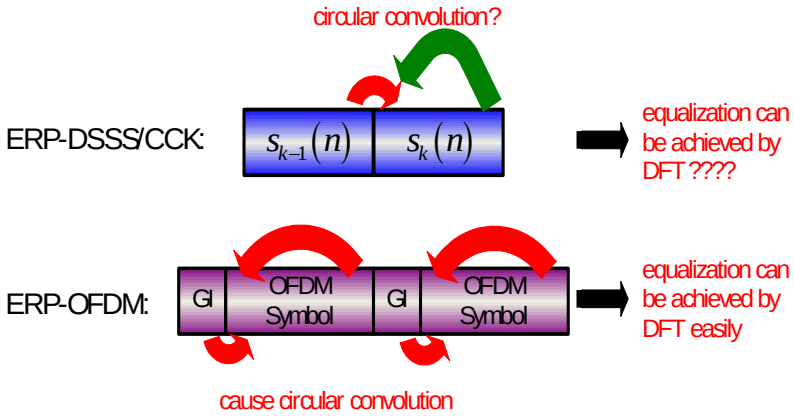

Although there have been already many frequency domain deconvolution techniques [7], they are still not suitable in our situation because multipath may be composed of severe selective fading and unstable poles instead of convergent filtering. Besides, these existing frequency domain method over time domain signal require 2 or more FFT blocks, which means more hardware cost, and since frequency responses

resulted from these methods contain aliasing due to non-circular convolution, we cannot design a frequency domain CCK demapper based on them. Another issue is the problem of traditional one-tap equalization, which noise would be enhanced largely on very deep channel frequency response. Unlike OFDM system where signal is modulated to fixed magnitude for each frequency, every possible DSSS codeword has its own different frequency response, and that makes such effect vary so significantly among DSSS symbols that the performance is unpredictable and bounded by transmitted sequences while it has actually been improved greatly in [8],

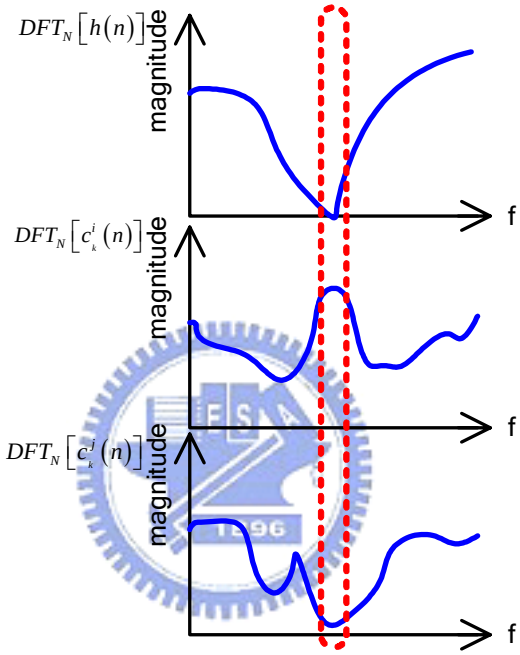

[9] and [10]. As a result, we are going to propose a novel frequency domain approach to overcome aliasing caused by FFT and deal with DSSS equalization and CCK demapping, and at the same time, the processes are completed by sharing OFDM equalization blocks. Note that it is well known and discussed broadly for OFDM channel estimation and equalization so the remaining of this thesis would focus on how to solve difficulties in DSSS mode under our receiver block diagrams and requirement.

Chapter 3

Channel Estimation & Equalization

According to proposed receiver block diagrams, we hope to seek frequency domain techniques to handle the originally time domain signal. These concepts are indeed considered and discussed a lot in recent years and combined with adaptive filters further. Frequency domain processes have primarily advantages compared to time-domain implementations. The first advantage is the potentially large savings in computational complexity because of block-based signal processing. The FFT is an efficient implementation of the DFT that provides this advantage. The second is that the DFT and the filter bank structures generate signals that are approximately orthogonal. In addition, this technique applied to DSSS signals in our approximately universal receiver reuses equalization modules of OFDM mode. Now we are going to show proposed relative schemes—channel estimation and equalization—that are very different from general adaptive methods [7].

3.1 Channel Estimation

The most common approach for coefficients estimation is usually adaptive algorithm that need not rely on specific data format and conditions. Least mean squares (LMS), recursive least squares (RLS), DFE, etc are famous and widely-used time domain adaptive methods to calculate the channel impulse responses over DSSS system. Even if the ideal coefficients may be not obtained by practical process for some conditions, that is, there exists no inverse, adaptive algorithm is able to approximate very closely. However, taking proposed receiver architecture into account, expected estimation scheme should be realized in frequency domain

instead of time domain, and that results in challenges indeed. One idea is just to transform the processes of adaptive algorithms applied in time domain to frequency domain, and it has been done based on RLS algorithm in [11] with mathematical deduction. Another is to make use of overlap-and-save and overlap-and-add technique with adaptive loops [7]. Though FFT is convenient to deal with and to reduce convolution over time domain, approaches mentioned above need additional operations and IFFT to eliminate aliasing attributed to non-circular convolution. Here are two different methods in essence, simpler and non-adaptive ways that exploit the characteristics of spreading codes resulting (pseudo) circular prefix and the concepts of fast linear convolution by means of Fourier transform. The first one, in fact, is to find the condition that satisfies circular property; the other is to use common FFT technique and is unconcerned with circular property. The comparison between these two schemes will be shown along with proposed equalizer in chapter 5. And no matter which one is better, each provides a possibility of frequency domain channel estimation over DSSS system.

3.1.1 Proposed Scheme #1

Guard interval of OFDM system is a cyclic extension of the symbol, repetition of tail part of the symbol so equalization can be achieved easily in frequency domain. Well, where is the circular prefix during DSSS preamble?

If we do not considering the length of FFT window, two successive identical spreading sequences can meet our requirements; that is, the former is regarded as the circular prefix of the latter. Notice that the length of spreading code in this case is equivalent to the length of circular prefix, the maximum delay this format can suffer. Figure 3.1 illustrates that though spreading sequences are linear convolved with multipath, we can conduct the latter sequence as circular convolved with multipath under condition of two successive identical spreading sequences,

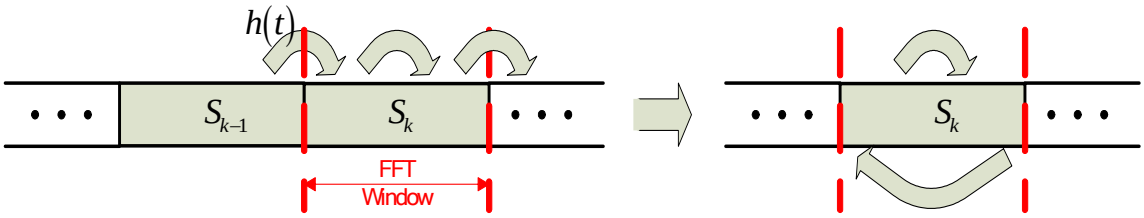

Figure 3.1 2 successive identical symbol lead to circular property

, where S_i is some spreading sequence, S_k is the same with the previous S_{k-1}, and the curved arrow represents multipath effect $h(t)$. Hence, if the maximum delay of $h(t)$ does not exceed the length of spreading code, the multipath channel frequency response $H(\omega)$, can be calculated easily by

$$H(\omega) = \frac{Y_k(\omega)}{S_k(\omega)} \tag{3.1}$$

, where $Y_i(\omega)$ is received signals that is the results of transmitted signal convolved with multipath effect, and $S_i(\omega)$ is the frequency response of spreading sequence S_i. Generally, in order to ensure detecting of packet and estimation of unideal factors, the modulation during preamble is usually simpler than that in data frame and, in other words, is with longer distance between code sets than modulation of data. As a result, this situation can occur frequently and easily during preamble of common DSSS system, and an estimation scheme can thus be developed based on such a simple concept.

There are still two improvements in algorithm itself: noise suppression of noise and enhancement of tolerance of multipath maximum delay. According to equation (3.2)

$$y(t) = x(t) \otimes h(t) \otimes S_{PN}(-t) = h(t) \otimes \left[x(t) \otimes S_{PN}(-t) \right] \tag{3.2}$$

, we can employ the technique on transmitted signal as well as on correlation output with PN code, $x(t) \otimes S_{PN}(-t)$, to obtain channel frequency response. This concept is similar to the use of spreading sequence to raise SNR; that is, to reduce noise relatively. For limitation of multipath length, unlike initial consideration of one symbol as circular prefix, two or more symbols are taken into account, and the criterion depends on the specifications of platforms, standard requirements, or environments. Finally, a general process chart is carried out as following Figure 3.2.

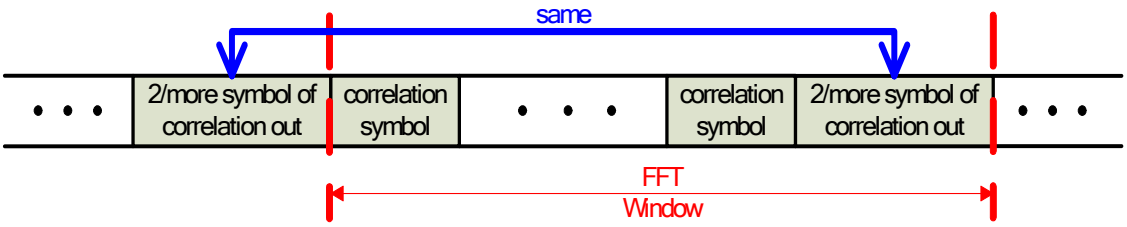

Figure 3.2 consideration of multiple symbols

For example of IEEE 802.15.4 [12], the preamble field is composed of 32 binary zeroes, and each 4 zeroes of them will be spread by only one 32-chips long PN sequence. If the length of FFT window is 32, merely one spreading sequence will be included and if it is 64, two is consider. And with increase of FFT window, the tolerance of multipath maximum delay and the precision of estimation are stronger and sharper also.

This concept is actually simple, but it is restricted by defined preamble format, and it seems to have some difficulty in our choice, IEEE 802.11g ERP-DSSS mode. The resources in proposed receiver for channel estimation are 64-point FFT that is equipped for OFDM system and 11-chips Barker sequence as the PN code for DSSS system. The number of FFT points decides the FFT window; the length of PN code, that of circular prefix. Under these constraints, the only problem is that the length of FFT is not multiple of the length of Barker sequence, and one ($11\times3-32=1$) or two ($11\times6-64=2$) chips of the last symbol in FFT window must be cut off so the condition of circular prefix can no longer be achieved easily. However, because the characteristics of Barker codes are almost mutual irrelevant except totally matching between received signals and prepared barker correlator, the correlation output will be stable excluding the occurrence of correlation peak, seeing Figure 3.3.

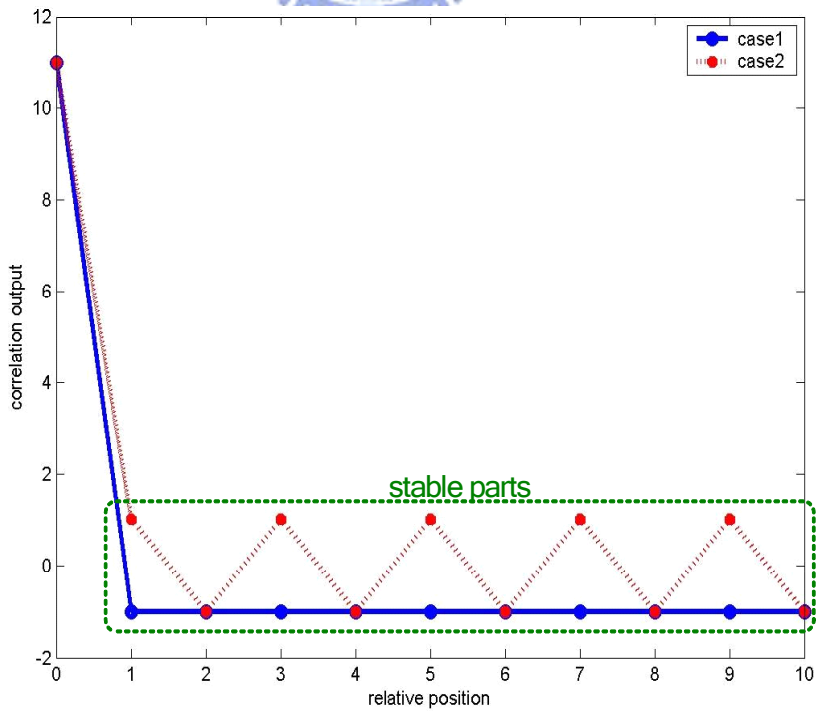

Figure 3.3 features of correlation over 11M Hz

Even though some correlation chips has to be cut, the remaining of stable parts resemble the stable parts in front of referenced FFT window, and those chips can still result in “pseudo” circular property. As a result, channel estimation has no need to adopt additional IFFT because of adaptive algorithms and can be accomplished by equation (3.1) again even if the preamble of 802.11g ERP-DSSS/CCK mode has no prepared format for frequency domain operation. The numbers of cut-off chips are one for 32-point FFT window and two for 64-point FFT window, so the length of pseudo circular prefix is consequently nine for 32-point FFT and eight for 64-point FFT (only stable parts, 10 chips, are able to produce circular condition).

Estimation condition mentioned above is illustrated in Figure 3.4, and Figure 3.5 is data flow of scheme #1 combined with OFDM equalization, which the intersection of yellow block and green block stands for sharing parts. Figure 3.6 is the estimation result under a randomly generated IEEE multipath model with RMS delay 100 ns and SNR 7 dB by means of 64-point FFT. Note that the sampling rate is 11M Hz per second, i.e. sample time, T_s, is 90.9 ns and so multipath model does. Proposed scheme #1 endures at most nine chips long multipath fading. Clearly, the first eight estimated multipath impulse responses almost reach the ideal ones to some extent in Figure 3.6. Though maximum delay of multipath model we used exceeds what scheme #1 can bear, the excess multipath tails influence so slightly that estimation errors of excess parts are still small enough. The estimation result will also be supported by simulation result in chapter 4 with proposed equalization and demapper.

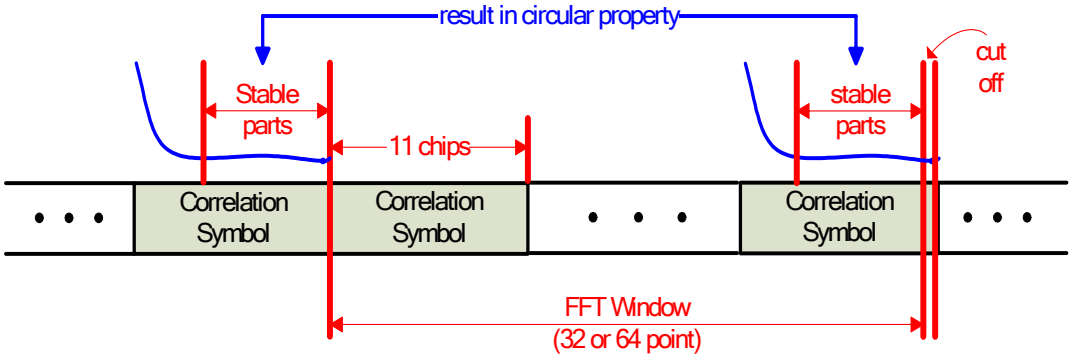

Figure 3.4

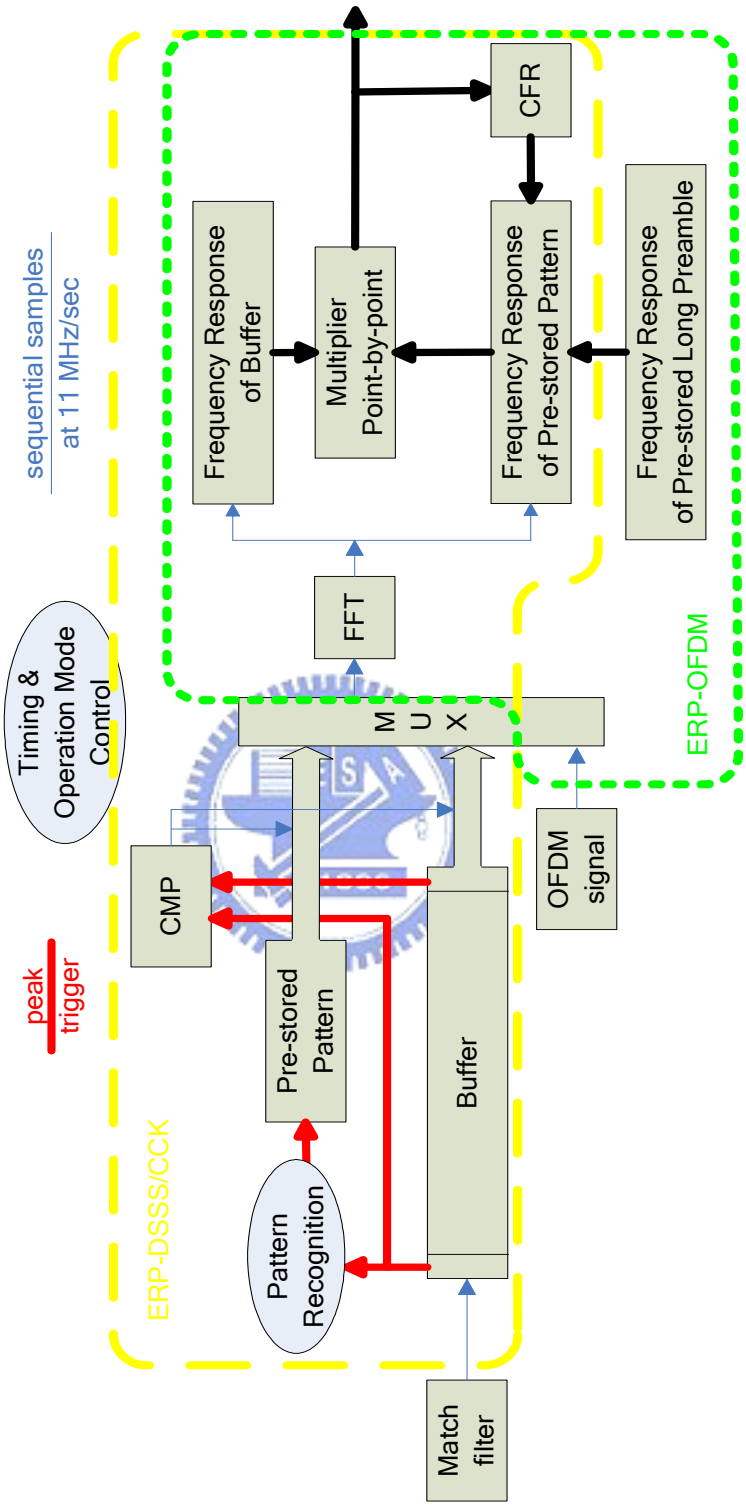

Figure 3.5 data flow of proposed scheme #1 channel estimation combined with OFDM channel estimation

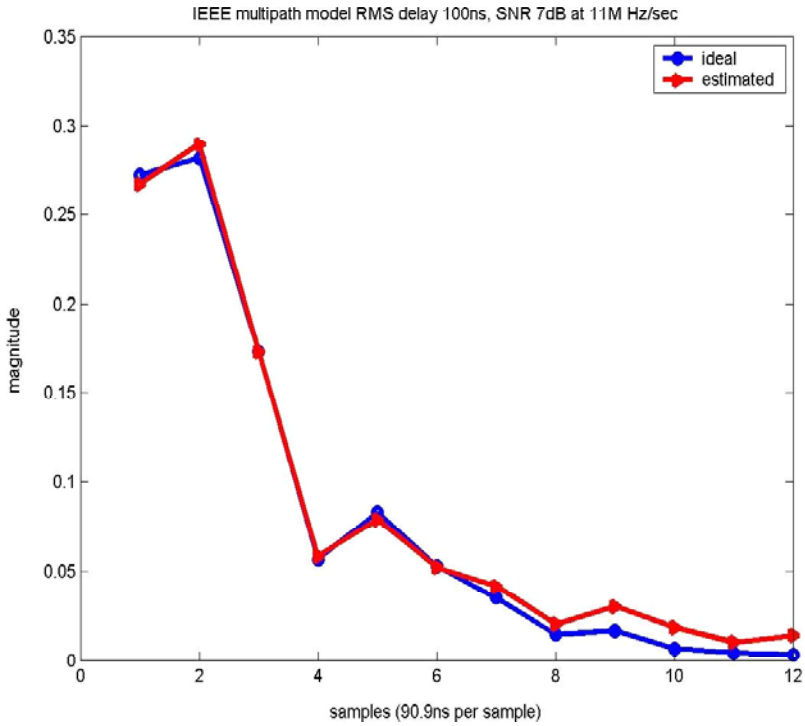

Figure 3.6 estimation result of scheme #1 and ideal CIR over 11M Hz

However, regarding the large excess delays of the JTC channels and multipath spacings shorter than sample time, such method operating at symbol rate is not feasible since the resolution is too low to react the channel impulse response. In contrast to the symbol rate estimator, a fractionally-spaced process is based on sampling the incoming signal at least as fast as the Nyquist rate. In facts, most equalizers that have outstanding performance are with at least $T_s/2$ -spacing or even smaller spacing, and it means 22 MHz or higher sampling rate is needed in our design. New problem appears. Figure 3.7 is correlation cases with 22 MHz sampling. Unlike Figure 3.3, it has a sub-peak at last and it explains why the same technique no longer works at 22 MHz. After cutting off in FFT window, the sub-peak will be taken away, but the correlation chips originally regarded as pseudo cyclic prefix still keep the sub-peak. When operating rate of estimator is increased to 22 MHz, the correlation property originally used to produce pseudo circular condition over Barker code sampled at 11 MHz is destroyed over Barker code sampled at 22 MHz. How large the estimation error would consequently be is shown in Figure 3.8, and the influence will also be proven by simulation results. For higher sampling rate, it seems that we need a more robust, accurate estimation scheme.

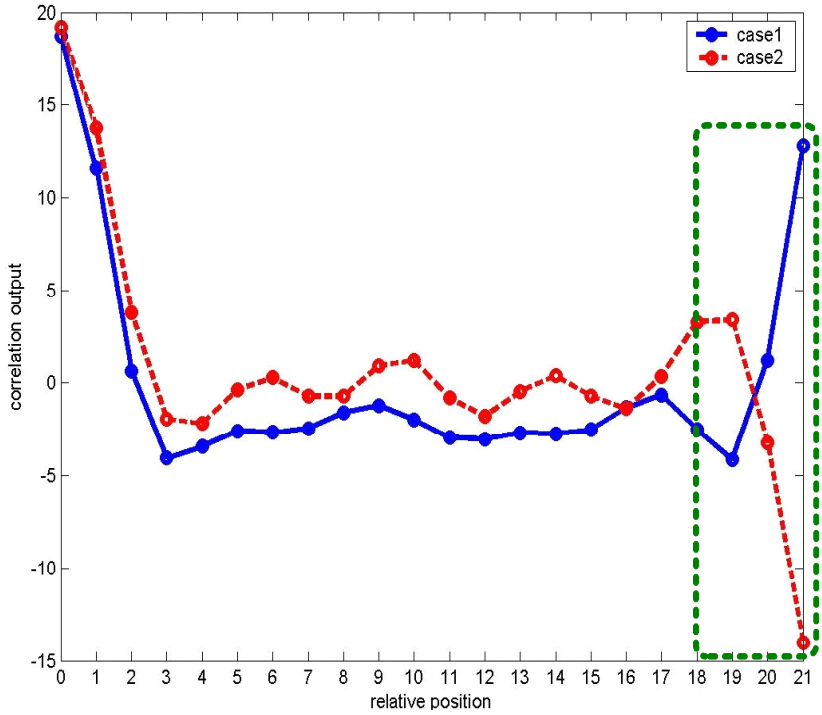

Figure 3.7 features of correlation over 22M Hz

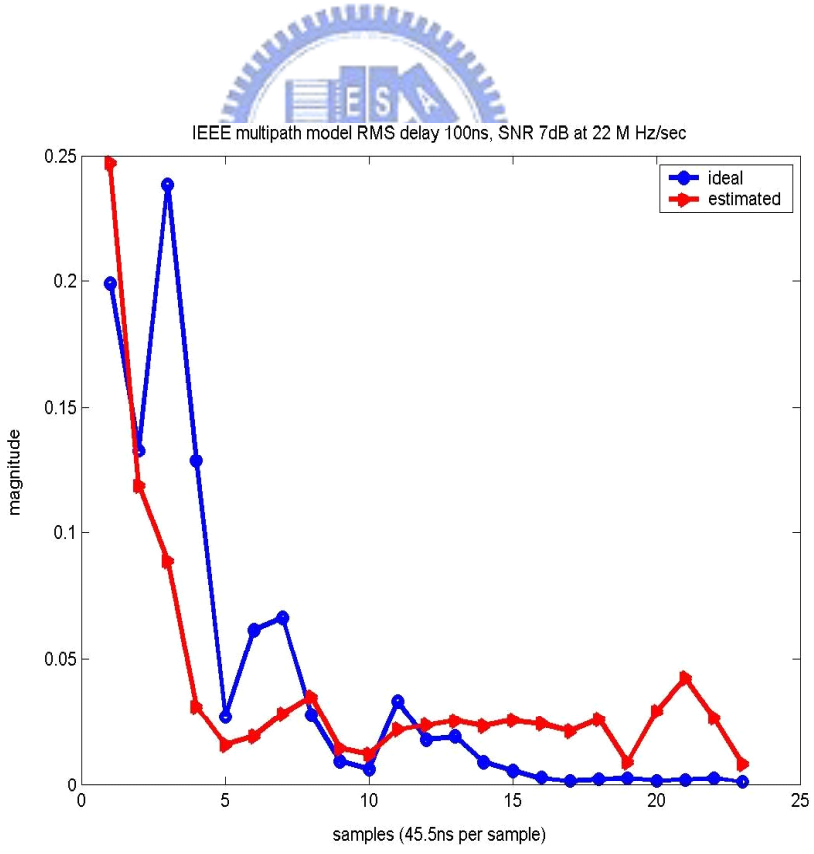

Figure 3.8 estimation result of scheme #1 and ideal CIR over 22M Hz

3.1.2 Proposed Scheme #2

Different from the previous algorithm, this one is based on well-known FFT technique, fast linear convolution. The linear convolution of two finite sequences is commonly performed by extending the input sequences with zeroes to length 2N, and then evaluating the circular convolution of these two sequences using FFT. Because the architecture of FFT adopted here is 2-radix and is easily adjustable for power-of-2 FFTs, such as 16, 32 or 64 points in our simulation platform, N is the smallest power of two greater that or equal to the longer one of two input sequence. Consider the linear convolution $\{c(n), 0 \le n < N_a + N_b - 1\}$ of two finite $\{a(n), 0 \le n < N_a\}$ and $\{b(n), 0 \le n \le N_b\}$:

$$c(n) = \sum_{0 \le i < N_a; 0 \le j < N_b; i+j=n} a(i)b(j) \qquad 0 \le n < N_a + N_b - 1 \tag{3.3}$$

Define the 2N-point vectors a_1, b_1 and c_1,

$$a_1 = [a(0) \cdots a(N_a - 1)\ 0^T_{2N-N_a-1}]^T \quad ; b_1 = [b(0) \cdots b(N_x - 1)\ 0^T_{2N-N_b-1}]^T$$
$$c_1 = [c(0) \cdots c(N_a + N_b - 2)\ 0^T_{2N-N_a-N_b}]^T ; (0_v \text{ is the zero conlum vector of length } v)$$

Therefore, c_1 can be written as the linear convolution in form of matrix operation,

$$c_1 = \begin{bmatrix} a_1[0] & 0 & 0 & \cdots & 0 \\ a_1[1] & a_1[0] & 0 & \cdots & 0 \\ a_1[2] & a_1[1] & a_1[0] & \cdots & 0 \\ \vdots & & & & \\ a_1[2N-1] & a_1[2N-2] & a_1[2N-3] & \cdots & a_1[0] \end{bmatrix} \cdot \begin{bmatrix} b(0) \\ \vdots \\ b(N_b - 1) \\ 0 \\ \vdots \\ 0 \end{bmatrix} \tag{3.4}$$

Because of zeroes padding in later half of a_1 and b_1, the above equation can also be written as circular convolution:

$$c_1 = \begin{bmatrix} a_1[0] & a_1[2N-1] & a_1[2N-2] & \cdots & a_1[1] \\ a_1[1] & a_1[0] & a_1[2N-1] & \cdots & a_1[2] \\ a_1[2] & a_1[1] & a_1[0] & \cdots & a_1[3] \\ \vdots & & & & \\ a_1[2N-1] & a_1[2N-2] & a_1[2N-3] & \cdots & a_1[0] \end{bmatrix} \cdot \begin{bmatrix} b(0) \\ \vdots \\ b(N_b-1) \\ 0 \\ \vdots \\ 0 \end{bmatrix} \quad (3.5)$$

Consequently, the FFT of c_1, C_1, is directly multiplied by the 2N-point FFTs of a_1 and b_1, A_1 and B_1 respectively, term by term.

$$C_1[s] = A_1[s] \cdot B_1[s],\ A_1[s] = \frac{C_1[s]}{B_1[s]},\ \text{or } B_1[s] = \frac{C_1[s]}{A_1[s]} \quad (3.6)$$

In other words, linear convolution or deconvolution process can be accomplished fast by frequency domain multiplication or division, which does not require circular property by zeroes padding technique. Undoubtedly, the technique is very useful for a system without special design against ISI, like DSSS system, and we attempt to replace a and b with multipath channel impulse response and spreading sequence respectively.

The key issue is that such technique is only for linear convolution of two “finite” sequences; yet, signal transmission is continuous symbol by symbol. Concerning every received symbol, it is interfered by previous symbol and resulted interferences that exceed one symbol length will last to next symbol. A complete linear convolution of a spreading sequence and multipath cannot be obtained. If the received symbol can be reconstructed to pure convolution result of referenced sequences, channel will be estimated easily.

Now, let $s_k(n)$ be the kth spreading symbol with length L_s, and H,

$$H = \begin{bmatrix} h_1[0] & 0 & 0 & \cdots & 0 \\ h_1[1] & h_1[0] & 0 & \cdots & 0 \\ h_1[2] & h_1[1] & h_1[0] & \cdots & 0 \\ \vdots & & & & \\ h_1[2N-1] & h_1[2N-2] & h_1[2N-3] & \cdots & h_1[0] \end{bmatrix} \quad (3.7)$$

, be channel matrix composed of $h(n)$, $n=0\cdots L_h-1$, where $L_h \le L_s$ (the channel spans about 2 spreading symbols). Note that h_1 and $\overline{s_k}$ are 2N-long vectors of $h(n)$ and $s_k(n)$ with zeroes padding, where N is the smallest power of two greater that or equal to L_s. Moreover, the channel matrix can be broken up into two parts:

$$H_i = \begin{bmatrix} H(1:L_s,:) \\ 0_{(2N-L_s)\times 2N} \end{bmatrix}$$
$$H_n = \begin{bmatrix} 0_{(2N-L_s)\times 2N} \\ H(L_{s+1}:2N,:) \end{bmatrix} \Leftrightarrow H = H_i + H_n,\ and\ H_p = \begin{bmatrix} H(L_{s+1}:2N,:) \\ 0_{(2N-L_s)\times 2N} \end{bmatrix} \quad (3.8)$$

, where H_p can be regarded as the shifted version of H_n, and this representation is used to clarify effect caused by previous symbol and inter chip interference. At the same time, linear convolution can be thought as super-position of convolution of each fragment. We divided each linear convolution result of transmitted symbol and multipath into “body”, signals within one symbol length, and “ISI component”, effects on next symbol. Therefore, a receiving symbol $y_k(n)$, $n=0\cdots L_h-1$, that would be extended to vector form $\overline{y_k}$ by zero-padding can be illustrated as Figure 3.9, and its

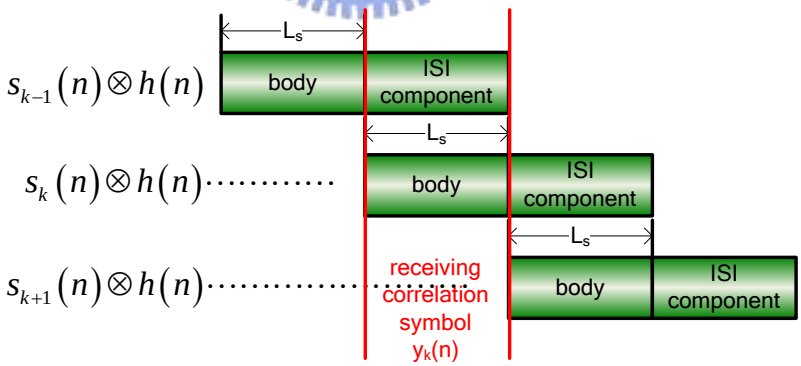

Figure 3.9

matrix equation can be correspondingly formulated as follows:

$$\overline{y_k} = H_i\overline{s_k} + H_p\overline{s_{k-1}} \quad (3.9)$$

In equation (3.9), the first term is the body from receiving symbol $\overline{s_k}$ and multipath,

and the second is the ISI component caused by previous symbol $\overline{s_{k-1}}$. For the purpose of reconstruction, we want to remove the ISI component attributed to previous symbol, and concatenating the ISI component that present symbol leads to and influence next symbol as shown in Figure 3.10.

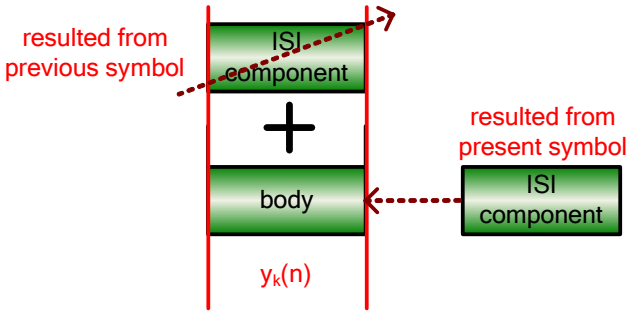

Figure 3.10

In vector expression, we can formulate above concept as

$$\begin{aligned}\overline{y_k} + H_n\overline{s_k} - H_p\overline{s_{k-1}} &= H_i\overline{s_k} + H_p\overline{s_{k-1}} + H_n\overline{s_k} - H_p\overline{s_{k-1}} \\ &= H_i\overline{s_k} + H_n\overline{s_k} \\ &= H\overline{s_k}\end{aligned} \tag{3.10}$$

, where the first L_s entries of $\overline{y_k}$ and $H_p\overline{s_{k-1}}$ are non-zero values, and the others are all zeros — this means they are signals or effects within one symbol length; on the contrary, the first L_s entries of $H_n\overline{s_k}$ are zeros, and the others are not — this represents ISI component. That is, after removing the ISI part attribute to last symbol ($-H_p\overline{s_{k-1}}$) and concatenating the ISI part that the present received symbol leads to ($+H_n\overline{s_k}$), the result will have the relation in equation (3.6), and thus, the channel frequency response can be worked out by the reconstructed result and detected $\overline{s_k}$.

So far, the only thing remained is how to Figure out $H_n\overline{s_k}$ and $H_p\overline{s_{k-1}}$. These two terms in essential stand for the same effect, ISI resulted from spreading sequence no matter $\overline{s_k}$ or $\overline{s_{k-1}}$. If we know the resulted ISI, we can do reconstruction by detected receiving spreading sequence. As far as DSSS mode in our platform is concerned, the preamble is modulated by DBPSK and spreading PN code is 11-chips Barker code. We denote the positive codeword — phase change 0 degree—spread by Barker code as $\overline{B}$, otherwise, the negative codeword—phase

change 180 degrees—as $-\overline{B}$. Receiving symbol $\overline{s_k}$ can be either $\overline{B}$ or $-\overline{B}$ as well as $\overline{s_{k-1}}$. Hence, let's consider two situations:

a) two successive $\overline{B}$:

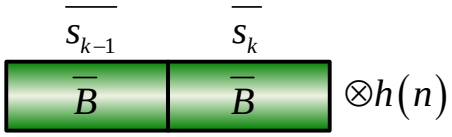

$\overline{s_k} = \overline{s_{k-1}} = \overline{B}$, and then substitute to equation (3.9). We have

$$\overline{y_k} = H_i \overline{B} + H_p \overline{B} \tag{3.11}$$

b) $-\overline{B}$ followed by $\overline{B}$:

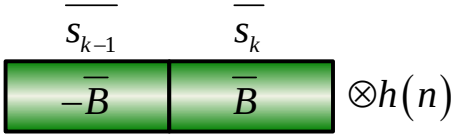

in this case, $\overline{s_{k-1}} = -\overline{B}$ and $\overline{s_k} = \overline{B}$. Similar to 1), we have

$$\overline{y_k} = H_i \overline{B} - H_p \overline{B} \tag{3.12}$$

The ISI component and body of $\overline{B}$ convolved with channel eventually can be obtained respectively by

$$H_p \overline{B} = \frac{Eq.\ (3.11) - Eq.\ (3.12)}{2} \tag{3.13}$$

and

$$H_i \overline{B} = \frac{Eq.\ (3.11) + Eq.\ (3.12)}{2} \tag{3.14}$$

, and so does for two successive $-\overline{B}$ and $\overline{B}$ followed by $-\overline{B}$. Such technique is inter-cancellation between different cases of signals, and it is able to be exploited not only for DBPSK but also for DQPSK or for other more complicated modulations (the larger code set is, the more complexity will be).

Consequently, let us summarize and introduce this algorithm to four steps in our platform:

a) Collect two sets of received spreading symbol:

One gathers or sums the symbols same with the previous one, and the other gathers or sums the symbols different from the previous one. By means of summation, noise can be suppressed.

b) Figure out the overall/average ISI component and body of $\overline{B}$ according to equation (3.13) and (3.14).

c) Reconstruction:
Use the result of b) to remove and concatenate the relative ISI components component based on different sets.

d) The multipath channel frequency response can be derived from

$$H_1 = \frac{F_{2N}(R)}{F_{2N}(\overline{B})} \tag{3.15}$$

, where R is the reconstructed result from c), F_{2N} is 2N-point DFT matrix, and H_1 is the Fourier transform of h_1 that is extended from $h(n)$ by zeroes padding.

Above steps are carried out in data flow Figure 3.9.

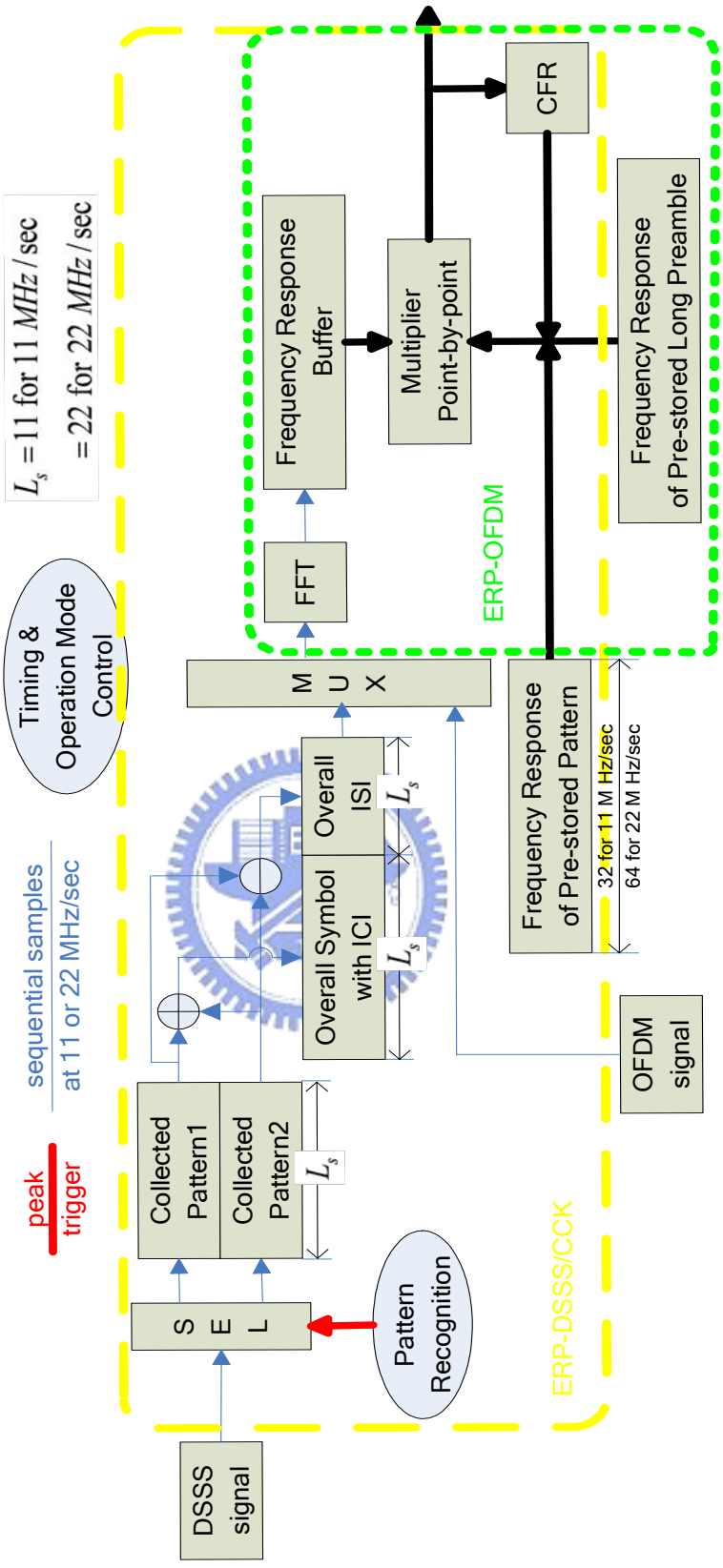

Figure 3.9 proposed scheme #2 channel estimation combined with OFDM channel estimation

The scheme is perform on platforms working at 11 MHz and 22 MHz for channel spacing 90.9 ns and 45.5ns respectively, as Figure 3.10 and Figure 3.11. They are simulated under a randomly generated IEEE multipath model with RMS delay 100 ns and SNR 7 dB by means of 32-point (N=16) FFT for the former, 64-point (N=32) FFT for the latter. We can obviously see that the accuracy of estimation result in Figure 3.10 is also very precise and the performance is almost the same with scheme #1 according simulation result. Moreover, scheme #2 is not restricted by sampling rate, that is, even if sampling is raised to 22 MHz, this algorithm is available, too. Although the accuracy under ISI resulted from transmit filter at sampling 22 MHz is still less than that at sampling 11 MHz, such estimation result can still make proposed receiver satisfy required system specs, remained to chapter 4, and prove the validation.

For advance consideration with longer multipath delay spread exceeding one spreading symbol length, scheme #2 can extend originally-considered one symbol spreading sequence to two or more ones against longer and more severe multipath, and then, the caused ISI to next two or more symbols can also be estimated by similar principle with more cases (more complicated algebraic equations).

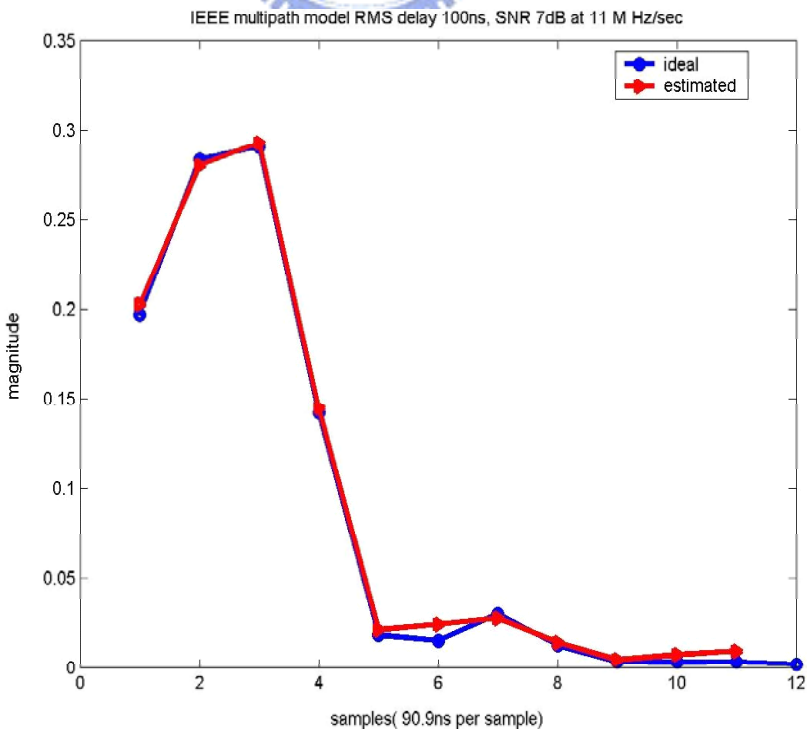

Figure 3.10 estimation result of scheme #2 and ideal CIR over 11M Hz

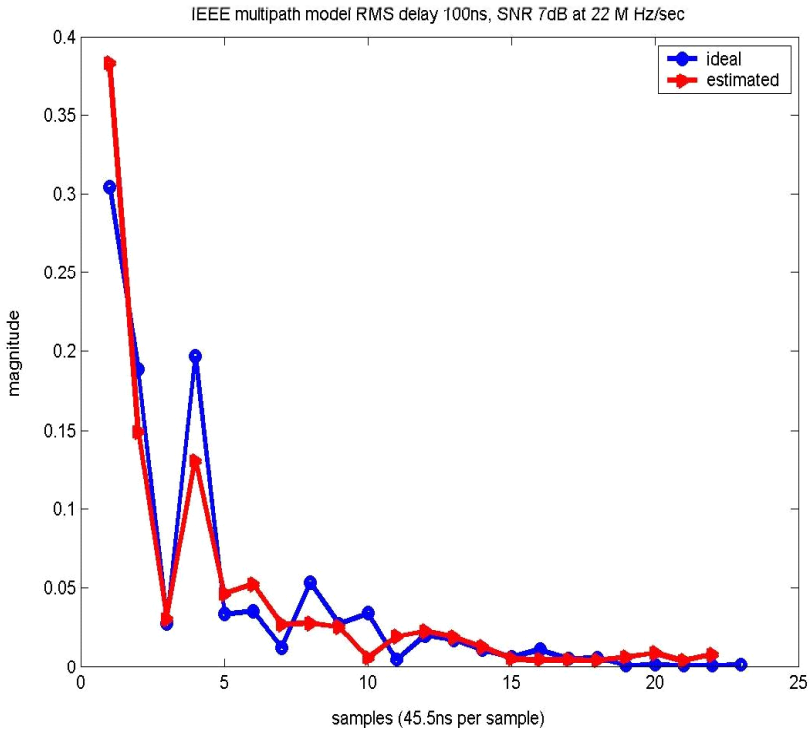

Figure 3.11 estimation result of scheme #2 and ideal CIR over 22M Hz

3.1.3 Comparison

The comparison for the two proposed estimation schemes is shown in Table 3.1. For consideration of 64-point FFT, scheme #1 has to keep 134 complex numbers (67 for received signals and 64 for recognized patterns) that prepare for channel estimation, but scheme #2 keep only 22 complex numbers for 11 MHz and 44 for 22 MHz, which both much fewer than scheme #1. Besides, scheme #1 is limited by barker PN code, and thus, it is specific and only suitable operating rate 11 MHz. On the contrary, because the process of scheme #2 construction is irrelevant to operating rate and spreading sequence, it is more general than scheme #1 and can be applied to other communication system based on spreading technique. Finally, the difference of performance will be simulated in chapter 4.

	Buffer Size	Operating Rate (MHz)	Flexibility
Scheme #1	134 complex numbers	11	specific
Scheme #2	22 complex numbers for 11 MHz 44 complex numbers for 22 MHz	11n (n: positive integer)	general

Table 3.1 comparison table for two channel estimation schemes

3.2 Equalization

3.2.1 Previous Remark

Equalization defined here is deconvolution or removes of multipath interference from received signal. As far as deconvolution is concerned, adaptive signal processing in time or frequency domain is widespread interest, but it is has potential problems with algorithm instability, convergence time consideration, and local minima. Therefore, combined with sharing concept, the initial direction for our design is frequency domain and non-adaptive equalization.

Overlap-and-save and over-and-add are two general methods. Since the product of two DFT sequences yields a circular convolution, this is not acceptable if the desired result is a linear convolution. Nevertheless, it can be shown that certain elements of the circular convolution correspond to a subset of the linear convolution, the size of which depend on the relative lengths of the two sequences. By overlapping elements of the data sequences and retaining only a subset of the final DFT product, a linear convolution between a finite sequence, channel impulse response here, and an infinite sequence, transmitted signal, is readily obtained. That's the origin of Overlap-and-save and over-and-add. But, the rule holds only on "convolution". Because no one can guarantee the non-singularity of impulse responses, there does not exist inverse operation; that is, we can only approximate the relevant coefficients for deconvolution without existence of inverse. This has been proven in [12] that the error component often appears as artificial oscillations and is possible very large or small. Also, not only this implies but also the simulation result supports that the system performance is bounded at some level.

3.2.2 Frequency Domain Equalization Combined with Data Demapping

Traditional equalization approaches separate equalization and CCK decoding, and are limited in performance especially when a DFE is used, due to error propagation in the feedback filter. Integrating problems mentioned before, we try an opposite train of thought; consider convolution instead of deconvolution. Now, we attempt to develop a joint equalization algorithm that demodulation is conditional on estimated channel impulse response before. The concept of joint equalization has

been realized by different algorithm in [13] and [14], and been presented demonstrating the greatly improved performance attained using this algorithm to the performance obtained using separate equalization and decoding block. So, the code set used to demodulation is, in the beginning, convolved with channel, and that is the place we claim that it is convolution-directed instead of deconvolution, and it is also called “joint equalization and decoding” or “combined equalization and decoding” in [13] and [14].

First, let $c_k^j(n)$, $0 \le n \le 7; 1 \le j \le 64$, is the received kth CCK symbol and belongs to the jth of 64 CCK symbol, and $h(n)$, $n = 0 \cdots L_h - 1$ is multipath impulse response with definition in equation (3.7) and (3.8). And $\overline{c_k^j}$ and h_1 are corresponding column vectors of $c_k^j(n)$ and $h(n)$ with extension of zeroes like section 3.1.2. So, the received vector $\overline{y_k}$, extended from $y_k(n)$, can be formed as

$$\overline{y_k} = H_i \overline{c_k^j} + H_p \overline{c_{k-1}^j} + N_k \tag{3.16}$$

,where N_k is zero-mean white complex Gaussian vector process with components of variance σ_n^2. For simplicity, assume that the last symbol is decoded correctly, and thus, the term $H_p \overline{c_{k-1}^j}$ can be removed in advance. So, the processed received vector $\overline{y_k}'$ we will face becomes

$$\overline{y_k}' = H_i \overline{c_k^j} + N_k \tag{3.17}$$

According to optimum maximum a priori (MAP) principle for transmission of CCK code words over ISI channel, the probability density function (pdf) $H_i \overline{c_k^j}$ conditioned on a hypothesis $\overline{y_k}'$ is

$$
\begin{aligned}
p(H_i\overline{c_k^j} \mid \overline{y_k'}) &\propto p(H_i\overline{c_k^j}) \cdot p(\overline{y_k'} \mid H_i\overline{c_k^j}) \\
&= p(H_i\overline{c_k^j}) \cdot \left[\prod_{k=1}^{n} 2\pi\sigma_n^2\right]^{-1/2} \cdot \exp\left[-\left\|(H_i\overline{c_k^j})^H \cdot \overline{y_k'}\right\|^2 \Big/ 2\sigma_n^2\right] \\
&\propto 2\,\mathrm{Re}\left[(H_i\overline{c_k^j})^H \cdot \overline{y_k'}\right] + \sigma_n^2 \ln p(H_i\overline{c_k^j}) - \left\|H_i\overline{c_k^j}\right\|^2
\end{aligned}
\tag{3.18}
$$

Without loss of generality, we assume 64 CCK code words are uniformly distributed, and equation (3.17) can be reduced to optimum maximum likelihood principle

$$
\begin{aligned}
p(H_i\overline{c_k^j} \mid \overline{y_k'}) &\propto p(H_i\overline{c_k^j}) \cdot p(\overline{y_k'} \mid H_i\overline{c_k^j}) \\
&\propto p(\overline{y_k'} \mid H_i\overline{c_k^j}) \\
&\propto 2\,\mathrm{Re}\left[(H_i\overline{c_k^j})^H \cdot \overline{y_k'}\right] - \left\|H_i\overline{c_k^j}\right\|^2
\end{aligned}
\tag{3.19}
$$

It is clear that the input signal, $\overline{y_k'}$, will be sent to the 64 correlators with coefficients $H_i\overline{c_k^j}$ and subtract power of each coefficients $H_i\overline{c_k^j}$ individually. Then, select the CCK code word with maximum correlation that means maximum possibility. However, not only the computation of coefficients $H_i\overline{c_k^j}$ and $H_p\overline{c_{k-1}^j}$ is large, but also they are almost kinds of time domain convolution (not really convolution). In order to reuse the equalization module of OFDM and avoid additional module that computes $H_i\overline{c_k^j}$ and $H_p\overline{c_{k-1}^j}$, we pass the received signal into DFT symbol by symbol. Equation (3.15) and (3.16) can be written as

$$
F\overline{y_k} = FH_i\overline{c_k^j} + FH_p\overline{c_{k-1}^j} + FN_k \tag{3.20}
$$

$$
F\overline{y_k'} = FH_i\overline{c_k^j} + FN_k \tag{3.21}
$$

, where F means 16-point (2 times length of CCK symbol) DFT matrix, and $FH_p\overline{c_{k-1}^j}$ can be removed as mentioned before. Especially, since Fourier transform is

a kind of linear transformation, FN_k is still a zero-mean white complex Gaussian vector process with a variance different from σ_n^2. Similar to equation (3.18), we can obtain a frequency domain maximum likelihood principle,

$$p(FH_i\overline{c_k^j} \mid F\overline{y_k}') \propto 2\,\mathrm{Re}\left[(FH_i\overline{c_k^j})^H \cdot F\overline{y_k}'\right] - \left\|FH_i\overline{c_k^j}\right\|^2 \tag{3.22}$$

And we can design a frequency domain ML demapper, which is composed of 64 correlators each with coefficient $FH_i\overline{c_k^j}$, based on this equation as Figure 3.12.

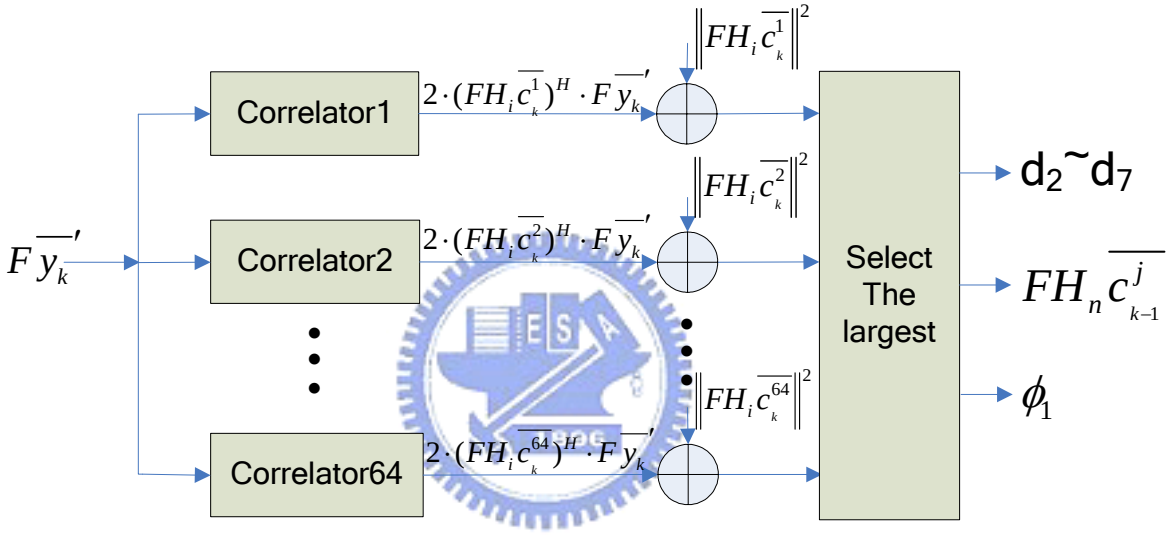

Figure 3.12 joint equalization decoder

Before going on, we clarify the remaining parts that are not solved. One is how to generate coefficients $FH_i\overline{c_k^j}$, which is used as coefficients for proposed demapper. The other is ISI term resulted from last CCK code word, $FH_p\overline{c_{k-1}^j}$, which is used to make received signal $F\overline{y_k}$ eliminate ISI effects and become $F\overline{y_k}'$. Review

equations (3.4)~(3.6) and (3.10), and multiply DFT matrix at two sides of equation (3.10),

$$FH\overline{c_k^j} = (Fh_1) \odot \left(F\overline{c_k^j}\right) = FH_i\overline{c_k^j} + FH_n\overline{c_{k-1}^j} \tag{3.23}$$

, where $\odot$ is direct multiplication entry by entry, Fh_1 is estimated channel frequency response, and $F\overline{c_k^j}$ is Fourier transforms of CCK code words. In equation (3.23), the first term $FH\overline{c_k^j}$ is the Fourier transform of linear convolution of channel impulse response and one CCK code word, and the right most two terms are frequency domain body, $FH_i\overline{c_k^j}$, and ISI component, $FH_n\overline{c_{k-1}^j}$. Therefore, what we need for ML demapper and ISI elimination is hided in $FH\overline{c_k^j}$, and it can be obtained by multiplication of Fh_1 and $F\overline{c_k^j}$. However, it is really a big problem to separate these two terms. Although they can be separated easily in time domain, our processing domain is frequency domain, and these two terms will be mixed due to Fourier transform.

Now we have to find a way to filter out these two terms in frequency domain.

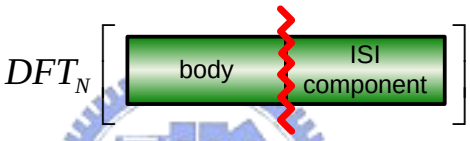

Regarding $H_i\overline{c_k^j}$, its first eight entries are the same with those of $H\overline{c_k^j}$, and the others are zeroes; so, $H_i\overline{c_k^j}$ can be rewritten as

$$H_i\overline{c_k^j} = GH\overline{c_k^j}, \quad G = \begin{bmatrix} I_{8\times8} & 0_{8\times8} \\ 0_{8\times8} & 0_{8\times8} \end{bmatrix} \tag{3.24}$$

We attempt to design an operator G', which can filter out $FH_i\overline{c_k^j}$ based on given $FH\overline{c_k^j}$ figured out from Fh_1 and $F\overline{c_k^j}$ such that

$$FH_i\overline{c_k^j} = G'FH\overline{c_k^j} \tag{3.25}$$

Combined with equation (3.24), we have a set of simultaneous equations, and the operator G' is introduced by

$$\begin{cases} H_i\overline{c_k^j} = GH\overline{c_k^j} \\ FH_i\overline{c_k^j} = G'FH\overline{c_k^j} \end{cases} \Rightarrow G' = FGF^{-1} \tag{3.26}$$

The other part, ISI component affecting next CCK symbol, can be derived from equation (3.23).

$$FH_n\overline{c^j_{k-1}} = FH\overline{c^j_k} - FH_i\overline{c^j_k} \tag{3.27}$$

Consequently, all information is generated for proposed frequency domain maximum likelihood decoder conditioned on CIR. Notice that although $FH_p\overline{c^j_{k-1}}$ is truly ISI component we want to remove when receiving a symbol instead of $FH_n\overline{c^j_{k-1}}$, $H_p\overline{c^j_{k-1}}$ is just a shifted version of $H_n\overline{c^j_{k-1}}$ in vector description. Each entry of $FH_p\overline{c^j_{k-1}}$ is equal to multiply each entry of $FH_n\overline{c^j_{k-1}}$ by $(-1)^{m-1}$, m is entry index, due to DFT, and it can also be achieved by changing sign bit on odd indices of vector $FH_n\overline{c^j_{k-1}}$.

After channel estimation is complete, processes are summarized as:

a) 64 sets of coefficients $FH_i\overline{c^j_k}$ and corresponding ISI effects can be computed sequentially according to equation (3.25) and (3.27), and at the same time, coefficients $FH_i\overline{c^j_k}$ are updated to correlators in Figure 3.12. This process will be finished before PSDU (CCK symbols) come.

b) As soon as the PSDU comes, the receiving CCK symbols will be sent into DFT first, and the result is $F\overline{y_k}$. Then, $F\overline{y_k}'$ is obtained by removing the ISI effect of past signal $FH_p\overline{c^j_{k-1}}$ from $F\overline{y_k}$.

c) $F\overline{y_k}'$ is fed into joint equalization demapper based on equation (3.22), and this demapper eventually outputs the most likely data bits and its ISI effect to feedback when next symbol comes.

Figure 3.13 is the corresponding data flow after timing synchronization, frequency synchronization, and channel estimation.

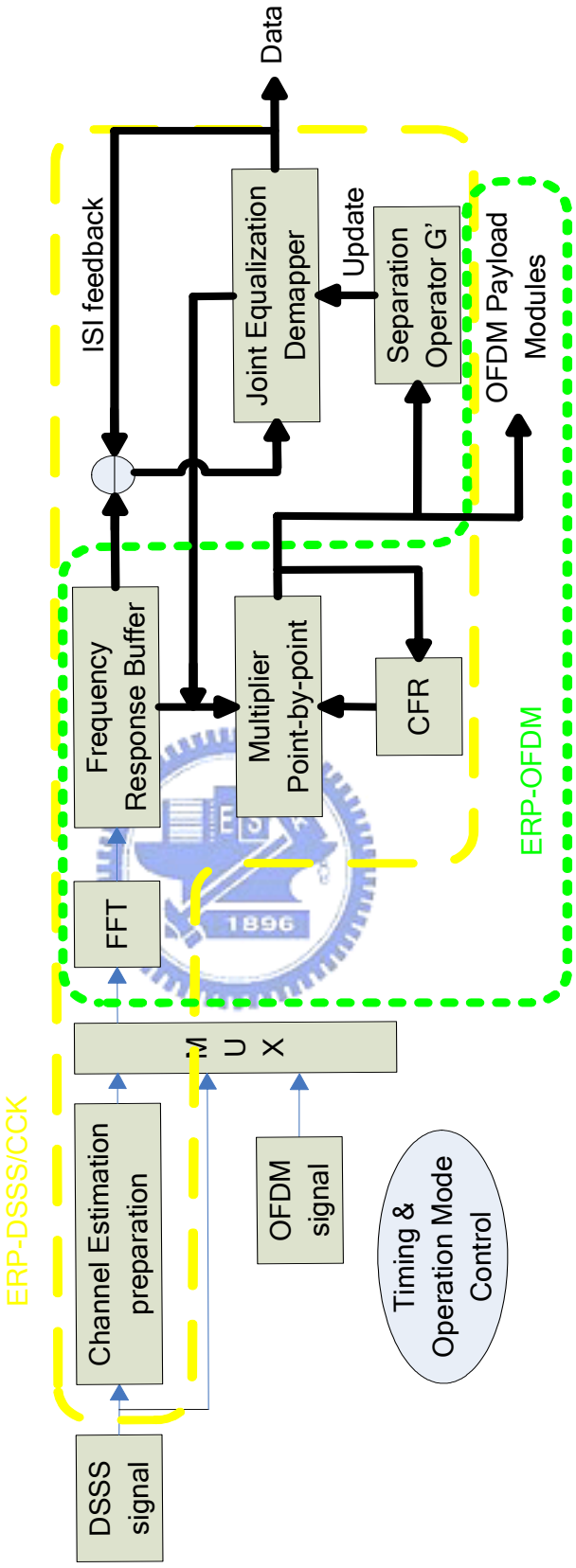

Figure 3.13 joint equalization data flow

So far, 16-point FFT was used because of the length of CCK symbol and applied FFT technique, and each resulted coefficient was sixteen long; i.e. the spacing is 90.9ns (11 M Hz/sc). However, it is insufficient to suffer from smaller spacing or severe multipath fading as mentioned in the beginning even if we can estimate correctly. For a given estimated channel at 22 MHz, the relative 22 MHz computations of coefficients, $FH_i\overline{c_k^j}$ and $FH_p\overline{c_{k-1}^j}$, are needed to react and resist against channel fading, but the results of $FH_i\overline{c_k^j}$ and $FH_p\overline{c_{k-1}^j}$ are not necessarily presented in 22 MHz, either. As general DFE structure, the feedforward equalizer is operated at 22 MHz (45.5ns-spaced), but the feedback equalizer is 90.9ns-spaced. The resulted difference from 11 MHz and 22 MHz is different correlator length. The correlator length at 22 MHz is two times as large as at 11 MHz, and two times hardware cost has to be taken into account. Thus, we try to implement $FH_i\overline{c_k^j}$ and $FH_p\overline{c_{k-1}^j}$ at both operating rate 11 and 22 MHz— correlator lengths will be 16 and 32 individually—for maximum likelihood demapper under receiver with 22 MHz sampling rate and do some analysis in chapter 4.

It is simple for consideration of 22 MHz $FH_i\overline{c_k^j}$ and $FH_p\overline{c_{k-1}^j}$ that all relative lengths of operations are merely doubled, and the separation operator G' becomes

$$G' = F_{32} G F_{32}^{-1}, \quad G = \begin{bmatrix} I_{16\times16} & 0_{16\times16} \\ 0_{16\times16} & 0_{16\times16} \end{bmatrix} \tag{3.28}$$

As to 11 MHz $FH_i\overline{c_k^j}$ and $FH_p\overline{c_{k-1}^j}$ derived from 22 M Hz computation, the lengths of prepared frequency domain CCK code words and DFT are, respectively, 16 (two times upsampled and it will be extended to 32) and 32 during coefficient computing, while the resulted coefficient length is maintain at 16 instead of 32 and incoming CCK symbol is received at 11 M Hz as well. This “down conversion” technique here lies in the operator G that produces separation operator G' again and is according to interpolation concept. Recalling an application of DFT signal processing, when we interpolate zero behind each element of $x(\bullet) = \{x_0, x_1, \cdots, x_{N-1}\}$, the Fourier transform of $x(\bullet)$ is equal to the first half of Fourier transform of $x'(\bullet) = \{x_0, 0, x_1, 0, \cdots, x_{N-1}, 0\}$

that is interpolated from x; that is,

$$X(k)=\sum_{n=0}^{N}x(n)e^{-j\left(\frac{2\pi}{N}\right)nk}=X'(k)=\sum_{n=0}^{2N}x'(n)e^{-j\left(\frac{2\pi}{2N}\right)nk},\ \text{for } k=0,1,\cdots,N-1 \quad (3.29)$$

For this reason, the separation operator G' is therefore designed as

$$G'=F_{32}GF_{32}^{-1},\quad G=\begin{bmatrix}\begin{bmatrix}1 & & & & \\ & 0 & & 0 & \\ & & 1 & & \\ & & & \ddots & \\ & 0 & & & 1 \\ & & & & & 0\end{bmatrix}_{16\times16} & & 0_{16\times16} \\ & 0_{16\times16} & & 0_{16\times16}\end{bmatrix} \quad (3.30)$$

As a result, the coefficients used for 11M Hz maximum likelihood demapper under 22 MHz receiver is obtained by retaining the first half after the output of separation operator G'. Worthy to notice that since we only need first half of the results of separation operator, the computation of separation are substantially the same with that under 11 MHz receiver. Although sampling rate and the process of separation are raised two times to 22 MHz, the hardware cost does not increase. Only half of information to be considered leads to performance loss definitely, and we will show how the loss is by simulation with kinds of channel models in chapter 4.

Ch4

Simulation Results

The packet error rate (PER) of two estimation methods with proposed demapper is regarded as our judgment and simulated under indoor channel models proposed by IEEE, JTC, and SPW with different RMS delays, different spacings of channel, and different sampling rate of receiver. The results presented in this section are carried out with ERP-DSSS/CCK 11 Mbps mode. We also assume a fading channel varying from packet to packet; i.e., it is constant within each packet, and the required performance is measured at a PER of 8%.

4.1 Channel Estimation Scheme #1 with Proposed Demapper

Figure 4.1 shows the performance in AWGN (dash line) and T-spaced (T=90.9ns) IEEE indoor channel model with different RMS delays (50ns, 100ns and 150ns), and the sampling rate of receiver is 11 MHz. Proposed scheme #1 can reach 8% PER before SNR 13 dB at most, and the results indicate that such estimation method is available and very good enough to resist multipath fading with 90ns spacing. But, this method cannot be extended to work at sampling rate 22 MHz with T/2-spaced channel taps. Figure 4.2 figures out that the estimation error caused by divergent correlation tail in Figure 3.6 affects the performance significantly, and the PER almost saturate at PER of 30%. For general purpose and against severe channel fading, scheme #1 is insufficient.

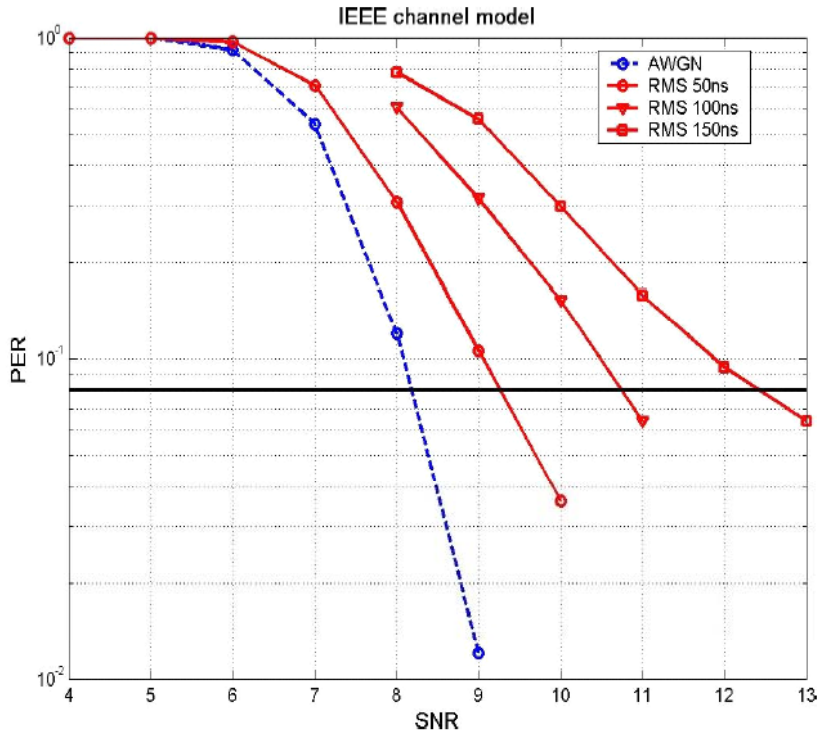

Figure 4.1 simulation results for AWGN and IEEE indoor channel mode at sampling rate 11 MHz

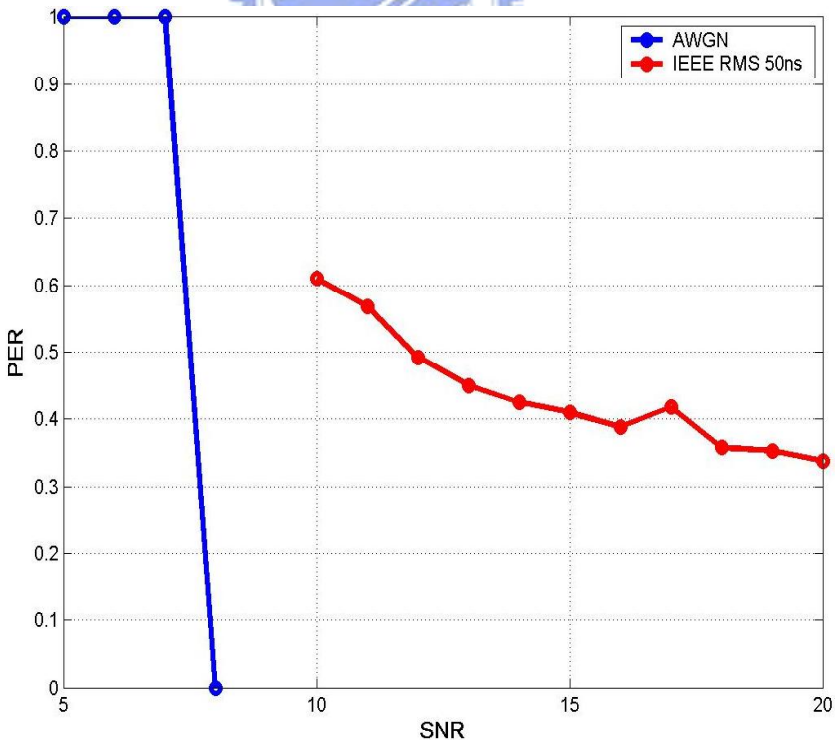

Figure 4.2 simulation results for AWGN and IEEE indoor channel mode at sampling rate 22 MHz

4.2 Channel Estimation Scheme #2 with Proposed Demapper

For estimation scheme #2, we directly simulate at operating rate 22 MHz with T/2-spaced channel taps to simulate. Addition to scheme #2 simulation, we arrange joint equalization demapper with two different rates, 11 MHz and 22 MHz. It is reasonable that the PER of 22 MHz demapper is better than 11 MHz demapper about 2.5 to 3 dB since the correlator length of 22 MHz demapper is twice as long as that of 11 MHz demapper as Figure 4.3 shown. In order to ensure proposed estimation scheme #2 can figure out equivalent CFR on samples even if large excess delays and multipath spacings unequal to multiples of sampling rate occurs, JTC indoor channel models are adopted. Similarly, we show simulation with different rate demappers separately in Figure 4.4 and 4.5. These results prove that proposed scheme #2 could react equivalent CFR not only for smaller spacing or server channel models but also for multipath not located on samples especially.

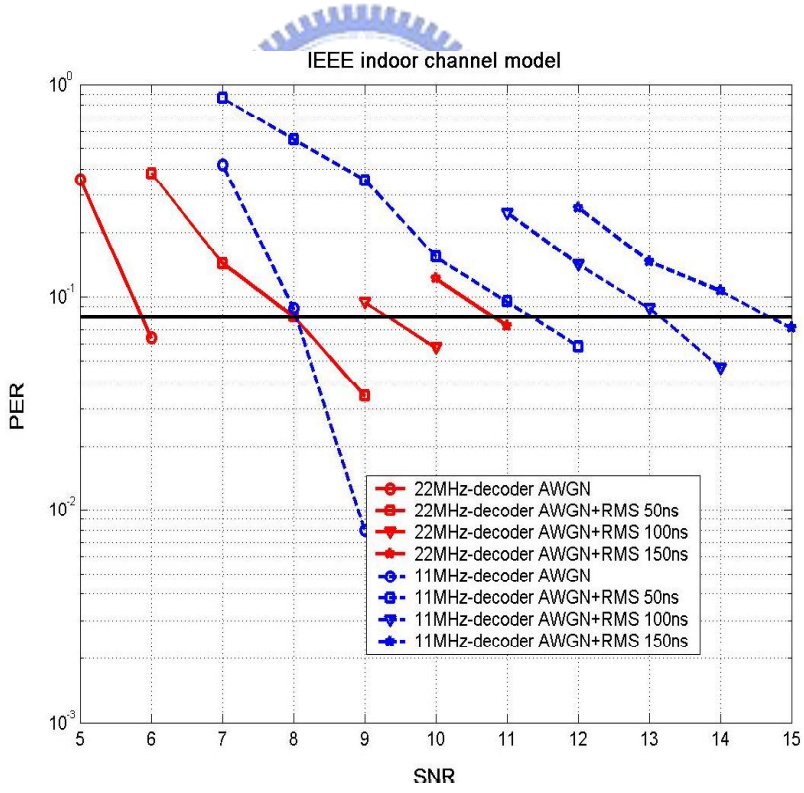

Figure 4.3 simulation results for AWGN and IEEE indoor channel mode at sampling rate 22 MHz

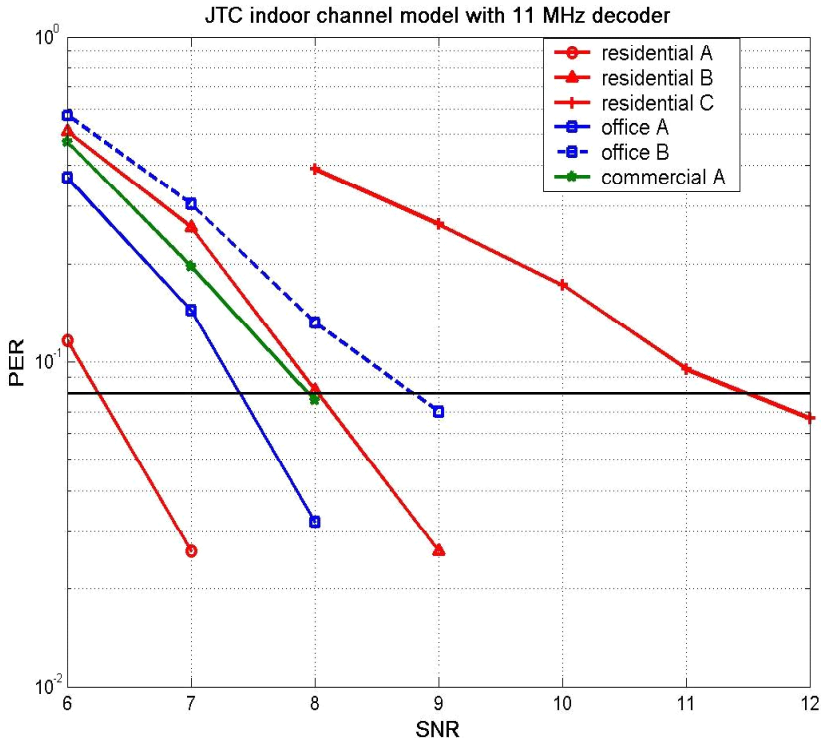

Figure 4.4 simulation results for JTC indoor channel model with 11 MHz demapper at sampling rate 22 MHz

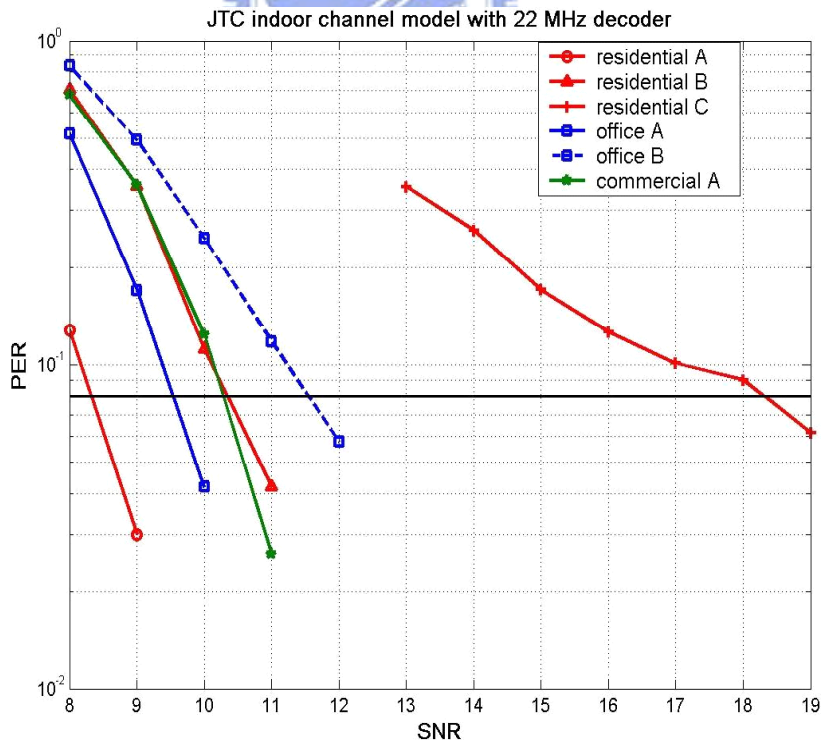

Figure 4.5 simulation results for JTC indoor channel model with 11 MHz demapper at sampling rate 22 MHz

Compared with [15] and [16], we can find that the combination of channel estimation scheme #2 and joint equalization demapper has improvement to some extent. In the case of JTC indoor office A, even 11 MHz demapper is about 4.5 dB better than [16] provides; in the case of JTC indoor residential C, although the PER of 11 MHz demapper is a little unusual, and it has to be made sure, the performance 22 MHz demapper can be equal or better than [16] at least.

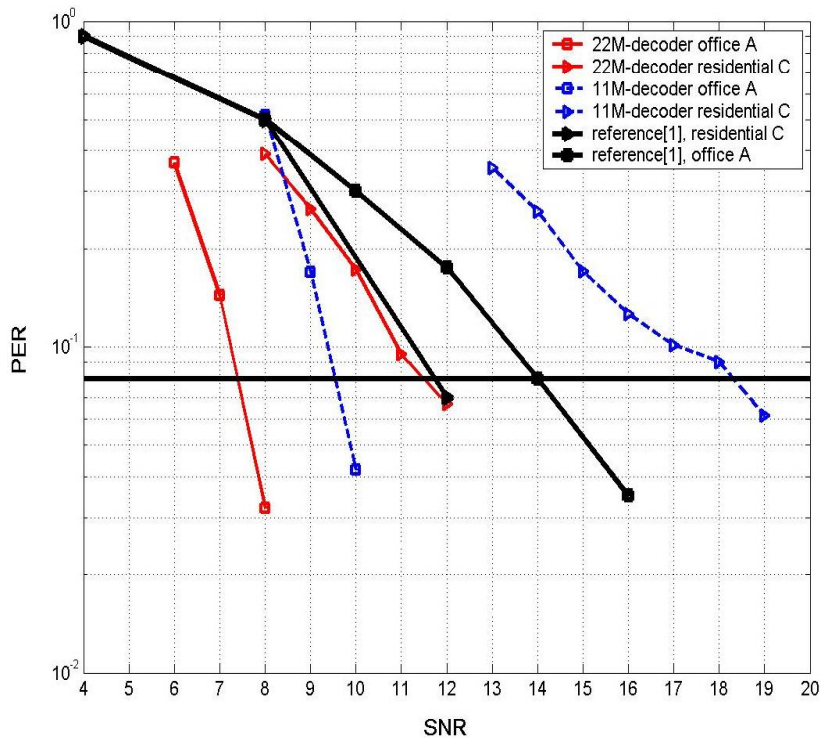

Figure 4.6 comparison with [1] for JTC indoor channel model residential C and office A

The reference PER curve in Figure 4.7 is fixed point simulation result with ADC 8 bits, and it provides a carrier frequency compensator that can tolerate CFO 50 ppm simultaneously. However, our simulations are floating point and without CFO consideration. According to [4], it is reasonable that we assume residual CFO, errors of frequency compensator, does not exceed 2 ppm. Although our results in Figure 4.7 are under float point, we still improve significantly even if we suppose that performance loss due to fixed point is about 1 dB.

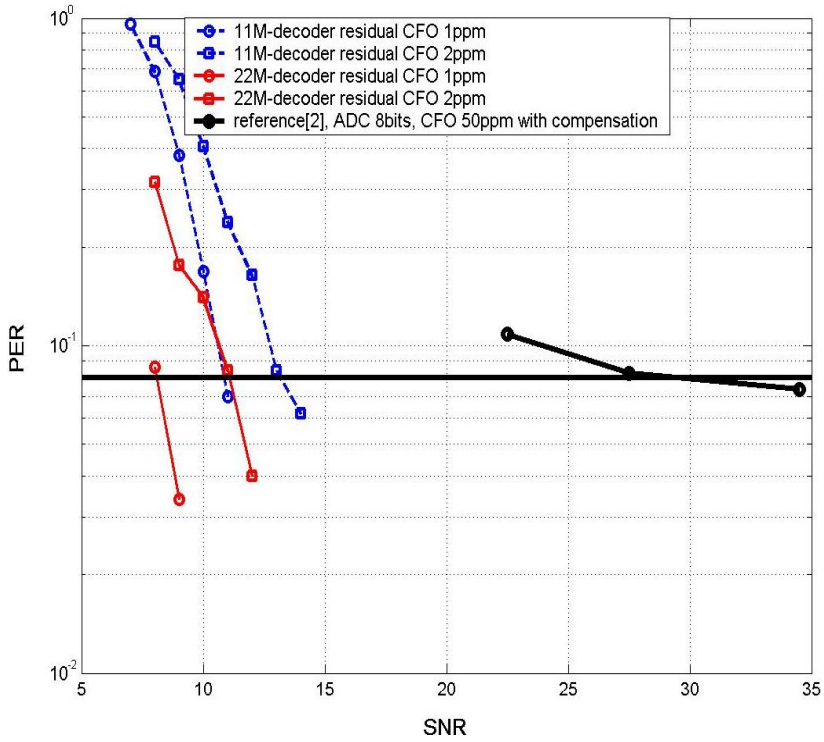

Figure 4.7 comparison with [2] for JTC indoor channel model residential B

Ch5
Conclusion and Future Works

5.1 Conclusion

The main contribution of this thesis is to provide and prove possibilities of frequency domain channel estimation and equalizer over DSSS system. Proposed processes overcome the difficulty of aliasing due to no cyclic prefix that is general in most frequency domain solutions by means of popular discrete signal processing, and can be applied to other DSSS system as well. They share the equalization modules in OFDM system so that they are suitable for dual mode communication system, IEEE 802.11g. With comparison to most solution to equalizer design, our design not only avoids additional and large DFE or adaptive algorithms but also reduces computation complexity whereby frequency domain one-tap multiplication. Most important, after integrating our method on 802.11g platform, our simulation results show further improvement and robustness against multipath fading from IEEE 802.11g indoor multipath model, SPW indoor multipath model and JTC indoor channel models even though considering reasonable residual CFO.

5.1 Future Works

Actually, compared our channel estimation and joint equalizer demapper with most approaches—DFE and FWT, our methods may not take advantage in hardware consideration. Although our estimation and equalization shares modules of OFDM mode, a maximum likelihood demapper that contribute to best performance is always the biggest one that all the others. The overall hardware cost cannot be therefore

reduced a lot. In the consideration of hardware cost reducing, we have two directions. To keep performance when we use 11 MHz demapper rather than 22 MHz demapper, designing a new separation operator is another issue so that we have performance of 22 MHz demapper but with shorter correlator length. Moreover, it is likely to decompose joint equalization demapper to a recursive one, and the correlation results can be pipe sequentially, like technique of FWT.

Finally, synchronization effects, like incorrect symbol timing and clock drift, will be bound into simulation for complete evaluation. Fixed-point simulation and HDL coding will also be accomplished to verify in chip level.

Bibliography

[1] IEEE 802.11b IEEE Standard for Wireless LAN Medium Access Control and Physical Layer Specifications, 1999

[2] IEEE 802.11a IEEE Standard for Wireless LAN Medium Access Control and Physical Layer Specifications, 1999

[3] IEEE 802.11g IEEE Standard for Wireless LAN Medium Access Control and Physical Layer Specifications, 2003

[4] Shih-Lin Lo, “The Study of Front-end Signal Process for Wireless Baseband Applications”, master thesis, June 2004

[5] Ming-Fu Sun, “”, master thesis, June 2005

[6] Ming-Ya Wu, “”, master thesis, June 2005

[7] Shynk, J.J, “Frequency-domain and Multirate adaptive filtering”, Signal Processing Magazine, IEEE Volume 9, Issue 1, Jan. 1992

[8] Wai-Kwong Yeung; Fan-Nian Kong, “Time domain deconvolution when the kernal has no spectral inverse”, Acoustics, Speech, and Signal Processing, IEEE Transactions on Volume 34, Issue 4, Aug 1986

[9] Zazula, D. “A method for the direct frequency-domain deconvolution without division”, Circuits and Systems II: Analog and Digital Signal Processing, IEEE Transactions on Volume 40, Issue 5, May 1993

[10] Zazula, D.; Gyergyek, L, “Direct frequency-domain deconvolution when the signals have no spectral inverse”, Signal Processing, IEEE Transactions on Volume 41, Issue 2, Feb. 1993

[11] Frank H. Hsiao, Terng-Yin Hsu, “A Frequency Domain Equalizer For WLAN 802.11g Single-Carrier Transmission Mode”

[12] Hansen, Per Christian, “Deconvolution and regularization with Toeplitz matrices”, Numerical Algorithm, 2002

[13] Ghosh, M , “Joint equalization and decoding for complementary code keying (CCK) modulation ”, Communications, 2004 IEEE International Conference on Volume 6, 20-24 June 2004

[14] Heegard, C.; Coffey, S.; Gummadi, S.; Rossin, E.J.; Shoemake, M.B.; Wilhoyte, M , “Combined equalization and decoding for IEEE 802.11b devices ”, Selected Areas in Communications, IEEE Journal on Volume 21, Issue 2, Feb. 2003

[15] Gerstacker, W.; Jonietz, C.; Schober, R, “Equalization for WLAN IEEE 802.11b ”, Communications, 2004 IEEE International Conference on Volume 6, 20-24 June 2004

[16] Barman, K.; Malipatil, A.V, “ICI equalizer in a CCK based DSSS communication system ”, TENCON 2003. Conference on Convergent Technologies for Asia-Pacific Region Volume 4, 15-17 Oct. 2003

Appendix

JTC indoor channel model profile

Indoor Office A RMS Delay Spread = 35 ns		
Tap	Delay (ns)	Avg Power (dB)
1	0	0
2	50	-3.6
3	100	-7.2

Indoor Commercial A RMS Delay Spread = 55 ns		
Tap	Delay (ns)	Avg Power (dB)
1	0	0
2	50	-2.9
3	100	-5.8
4	150	-8.7
5	200	-11.6

Indoor Office B RMS Delay Spread = 100 ns		
Tap	Delay (ns)	Avg Power (dB)
1	0	0
2	50	-1.6
3	150	-4.7
4	325	-10.1
5	550	-17.1
6	700	-21.7

Indoor Commercial B RMS Delay Spread = 150 ns		
Tap	Delay (ns)	Avg Power (dB)
1	0	-4.6
2	50	0
3	150	-4.3
4	225	-6.5
5	400	-3
6	525	-15.2
7	750	-21.7

Indoor Residential A RMS Delay Spread = 18 ns		
Tap	Delay (ns)	Avg Power (dB)
1	0	0
2	50	-9.4
3	100	-18.9

Indoor Residential B RMS Delay Spread = 70 ns		
Tap	Delay (ns)	Avg Power (dB)
1	0	0
2	50	-2.9
3	100	-5.8
4	150	-8.7
5	200	-11.6
6	250	-14.5
7	300	-17.4
8	350	-20.3